JPRS-JST-90-052
13 NOVEMBER 1990

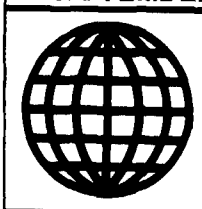

FOREIGN BROADCAST INFORMATION SERVICE

JPRS Report

Science & Technology

Japan

28TH CERAMICS SCIENCE DISCUSSION

JPRS-JST-90-052
13 NOVEMBER 1990

SCIENCE & TECHNOLOGY
JAPAN

28TH CERAMICS SCIENCE DISCUSSION

906C7512 Tokyo SERAMIKKUSU KISO KAGAKU TORONKAI in Japanese 24 Jan 90 pp 1-220

[Selected papers from the 28th Ceramics Science Discussion held 24-25 Jan 90 in Fukuoka, sponsored by the Japan Ceramics Association, the Chemical Society of Japan, and Kyushu Fine Ceramics Techno Forum]

CONTENTS

High-Performance α-Sialon Ceramics
[Masamichi Takai, Kenki Ishizawa, et al.]..... 1

High-Temperature Mechanical Properties, Internal Friction of Si_3N_4 Ceramics
[Yo Tajima, Kenichi Mizuno, et al.]..... 3

Effects of Some Mullites on Thermal Mechanical Properties of Al Titanate
[Akihiko Kawahara, Makoto Terasaki, et al.]..... 5

Strengthening ZrO_2 Ceramics by Thermal Stress
[Hiroshi Takada, Isao Tanaka, et al.]..... 7

Microstructure, Mechanical Properties of Al_2O_3 With Dispersed SiC Particles
[Keiji Matsuhiro, Yutaka Furuse]..... 9

Effect of Undercoating on Tensile Strength of SiC-Coated Carbon Fiber
[Kuniaki Honjo]..... 11

Superplasticity of Nonoxide Composites
[Fumihiro Wakai, Yasuharu Kodama, et al.]..... 13

Superplasticity of Hydroxyapatite
[Fumihiro Wakai, Yasuharu Kodama, et al.]..... 15

Fabrication of TiB_2–Ni Functionally Gradient Materials by Gas-Pressure Combustion Sintering
[Toshikazu Takahura, Isao Tanaka, et al.]..... 17

Some Properties of SiC–C Functionally Gradient Material Prepared by CVD
[Makoto Sasaki, Toshio Hirai, et al.]..... 19

Characteristics of Carbon Fiber Reinforced SiC Composite Fabricated Using Polysilazane
[Kikuo Nakano, Akira Kamiya, et al.]..... 21

Pressureless Sintering of SiC-Platelet Dispersed Si_3N_4 Composites
[Tatsuo Noma, Michael J. Hoffmann, et al.]..... 23

Preparation of SiC–Si_3N_4 Composite Powder From Si_3N_4 Mixture by YAG Laser
[Takeshi Okutani, Yoshinori Nakata, et al.]..... 25

Oxidation Behavior of Oxide/SiC-Whisker Composites
[Satoshi Iio, Hitoshi Yokoi, et al.]..... 27

Preparation of TiC–C Composite by Chemical Vapor Deposition
[Hiroyuki Suzuki, Makoto Sasaki, et al.]..... 29

Preparation of Ceramic Composite TiC/TiB_2 Having High Toughness
[Akira Kamiya, Kikuo Nakano, et al.]..... 31

Preparation of Alumina–Particulate Composites by Metal Infiltration Methods
[Junichi Hojou, Osamu Sagawa, et al.]..... 33

Interface Structure, Mechanical Properties of Si_3N_4 Nanocomposites
[Kansei Izaki, Katsuaki Suganuma, et al.]..... 35

High-Temperature Properties of MgO-Based Nanocomposites
[Koichi Niihara, Atsushi Nakahira, et al.]..... 37

HIP Sintering of Si_3N_4–SiO_2 Ceramics
[Jianren Zeng, Isao Tanaka, et al.]..... 39

Reaction Analysis of Combustion Synthesis--(1) TiC, TiB_2
[Osamu Yamada, Toshikazu Takakura, et al.]..... 41

Sintering of Ceramics by Self-Combustion Synthesis
[Takashi Shiono, Nobuyuki Komura, et al.]..... 43

Properties, Preparation of Porous Body of SiC
[Yushi Yamamoto, Yoshiyuki Miyaji, et al.]..... 45

Preparation, Morphology of Coil-Like Carbon Fiber Grown by CVD
[Masayuki Kawaguchi, Koji Nozaki, et al.]..... 47

Morphology, Spring Characteristics of Si_3N_4, Carbon Fiber
[Hiroshi Iwanaga, Seiji Motojima, et al.]..... 49

Dielectric Properties of BN-C Thick Films
[Shigenobu Yokoshima, Takashi Goto, et al.]..... 51

Microstructures of Transition Metal Nitride Films Prepared by CVD
[Hiroshi Funakubo, Nobuo Kieda, et al.]..... 53

Effects of Substrates, Holders on Preparation of Diamond by Plasma CVD
[Hisako Hirai, Youichi Yazaki, et al.]..... 55

Preparation of Rf-Sputtered Amorphous Aluminum Oxynitride Films
[Toichi Hanada, Masahiro Kobayashi, et al.]..... 57

No-Hysteresis Piezoelectric Actuator
[Hiroshi Asakura, Hiroshi Yamamura]..... 59

Microstructure, Dielectric Properties of Tungsten Bronze-Type Ceramics
[Yoji Ueda, Toshio Kimura, et al.]..... 61

Preparation, Properties of $Y(Ba_{1-x}St_x)_2Cu_4O_8$ Superconductors
[Takahiro Wada, Takeshi Sakurai, et al.]..... 63

Preparation, Superconducting Properties of $Y(Ba,La)_2Cu_4O_8$
[Takeshi Sakurai, Takahiro Wada, et al.]..... 65

Fabrication, Evaluation of Br-Sr-Ca-Cu-O Superconductors by Sol-Gel Method
[Kouichi Yamashita, Masayuki Nagai, et al.]..... 67

Synthesis of Ag-Added Bi-Pb-Ca-Cu-O Powder by Spray Drying, Superconductivity of Powder
[Hiroko Higuma, Mitsunobu Wakata, et al.]..... 69

Composition, Superconducting Properties of Y-Ba-Cu-O Film Prepared by CVD
[Akira Suhara, Hisanori Yamane, et al.]..... 71

Microstructure, Properties of High-Temperature Bi Superconducting Ceramics
[Toshihiko Nishida, Takashi Otsuka, et al.]..... 73

Addition of Silver Into Superconducting Oxide Ceramics
[Yasumichi Matsumoto, Yoshiaki Yamaguchi, et al.]..... 75

Determination of Oxygen Content of $YBa_2Cu_3O_{7-y}$ Superconductors
[Yoko Suyama, Mamoru Matsumoto, et al.]..... 77

Synthesis of Mullite From SiO_2 Powders-Al Salt Solutions
[Hiroyuki Nakamura, Yukiko Katae, et al.]..... 79

Preparation of γ-Alumina Thin Porous Membrane by Sol-Gel Method
[Tatsuya Okubo, Masayuki Watanabe, et al.]..... 81

Preparation of $LiTi_2(PO_4)_3$ By Sol-Gel Method
[Noboru Toge, Jishun Zhu, et al.]..... 83

Preparation of $ZrSiO_4$ Powder by Using Sol-Gel Method—Part 2
[Toshihiro Terazaki, Hidehiko Kobayashi, et al.]..... 85

Preparation, Crystallization of System SiO_2-TiO_2 Through Alkoxide Processes
[Shoji Kaneko, Satoshi Suzuki]..... 87

Properties of Titanium Oxide Formed by Hydrolysis of Titanium Alkoxide
[Tadashi Sasamoto, Sumie Enomoto, et al.]..... 89

Preparation of Porous Silica Glass by Sol-Gel Method
[Hiromitsu Kozuka, Jun Yamaguchi, et al.]..... 91

Synthesis of Al_2O_3-ZrO_2 Fibers With Organometallic Precursors
[Satoshi Kodama, Toshinobu Yogo, et al.]..... 93

High Performance α-Sialon Ceramics

906C7512 Tokyo SERAMIKKUSU KISO KAGAKU TORONKAI in Japanese 24 Jan 90 p 11

[Article by Masamichi Takai, Kenki Ishizawa, Nobuo Ayuzawa, and Akira Shiranita, Shingawa Refractory Co., Ltd., and Mamoru Mitomo, National Institute for Research of Inorganic Materials, Science and Technology Agency]

[Text] **1. Introduction**

α-Sialon, a solid solution of the α-Si_3N_4 type, has the generic formula Mx $(Si, Al)_{12}(ON)_{16}$, where M denotes the metal element immersed in the solid solution, with $0<x\leq2$, and comes in two forms depending on the solid solution compositions: one, called part-stabilized α-sialon, has α-sialon and β-Si_3N_4 coexisting, with $0<x<0.3$; the other, referred to as completely stabilized α-sialon, belongs to the single phase region of α-sialon, with $0.3<x<0.8$. With the mechanical property being superior in the part-stabilized region, as reported previously,[1] the authors investigated this part-stabilized region in more detail regarding the relevant composition and sintering method and showed improved performance of the material at high temperature.

2. Method of Experiment

With its solid solution composition for x fixed at the theoretical values of 0.2 and 0.15, α-sialon involving yttria was investigated. The starting materials of high purity Si_3N_4, AlN, and Y_2O_3 were mixed in ethanol with the ball mill, followed by drying, and then subjected to CIP (cold isostatic pressing) at 150 MPa to give the compact. The compact was then subjected to normal-pressure sintering for 5 hours under a nitrogen atmosphere and at a temperature of 1,700°C, followed by HIP (hot isostatic pressing) for 1 hour at 120 MPa and 1,700°C, to give a sintered compact. The sintered compact was assessed for its density, constituent phases, mechanical properties, and microstructures.

3. Results and Discussion

The density of part-stabilized α-sialon with the theoretical composition are hard to raise generally, with the relative density of the compact sintered at normal pressure being about 96 and 91 percent for x values of 0.2 and 0.15,

respectively. In the present investigation, the compact so sintered at normal pressure was then given an HIP treatment which has led to attainment of the theoretical density for the resulting compact and to the disappearance of air pores therein, as confirmed by microscopic observation. Table 1 presents properties of the HIPed sintered compact. Although the content of α-sialon depends on the quantity of yttrium immersed in the solid solution, the ratio of α-sialon to β-Si_3N_4 was sustained unchanged even after the HIP treatment insofar as the part-stabilized sialon region is concerned, which may conceivably have led to the firm compact of fine complex microstructure wherein isodiametric particles of α-sialon and columnar pieces of β-Si_3N_4 coexist. It can also be seen from Figure 1, which shows results of measurement for the modulus of elasticity at high temperatures, that the fall of the value at high temperature levels from that at normal temperature was limited; this, in turn, may possibly show that the amount of grain boundary phase, a factor that deteriorates relevant high-temperature characteristics, is limited. Control of the microstructure of α-sialon ceramics in the part-stabilized region, therefore, is advantageous in raising the material's performance and has promise for application in antithermal and antiwear materials and in high-precision components.

Table 1. Properties of HIPed α-sialon Ceramics

Quantity of solid solution	Density	α-sialon content (%)	Hardness (GPa)	Average three-point-bending test	
				Room temperature	1,200°C
0.15	3.23	20	16.5	1,250	950
0.2	3.24	45	18.0	1,400	900

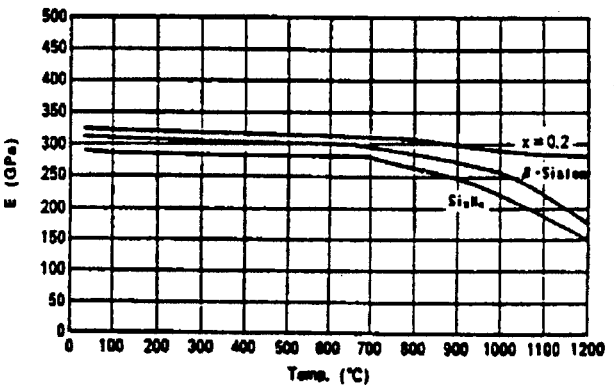

Figure 1. Plot of High-Temperature Young's Modulus vs. Temperature for α-Sialon Ceramics

References

1. JOURNAL OF JAPAN CERAMIC INSTITUTE, Vol 94 No 1, 1986, pp 183-185.

High-Temperature Mechanical Properties, Internal Friction of Si_3N_4 Ceramics

906C7512 Tokyo SERAMIKKUSU KISO KAGAKU TORONKAI in Japanese 24 Jan 90 p 12

[Article by Yo Tajima and Kenichi Mizuno, NGK Spark Plug Co., Ltd., and Kenichi Matsushita and Taira Okamoto, Sanken, Osaka University]

[Text] **1. Introduction**

High-temperature mechanical properties of Si_3N_4 ceramics depend largely on the chemical composition, microscopic structure, etc., of the materials in general. Addition of rare earth oxides to the ceramics, in this connection, provides a means of producing a composition displaying superior high-temperature characteristics and, further, a second metal oxide has often been added to the ceramics in combination with the former for improvement of its sintering properties, with the properties of the product actually influenced in large measure by the second addition. This article deals with an estimation of high-temperature mechanical properties and internal friction for a sintered ceramic, in which Al_2O_3 or Cr_2O_3 as well as Y_2O_3 was added as a promoter of the reaction, and with a study of the correlations of relevant compositions vs. relevant mechanical properties and internal friction.

2. Experiment

Measurements were taken on a hot-pressed sintered ceramic, YC, involving Y_2O_3 and CR_2O_3 as the promoters, and on a gas-pressure sintered ceramic, YA, involving Y_2O_3 and Al_2O_3 as the promoters, in the temperature range from room temperature to 1,400°C for three-point bending strength, for dynamic fatigue behavior, and, by using torsional vibration, for internal friction.

3. Results and Discussion

Results of measurement of strength and internal friction for the two kinds of sintered ceramics above are presented in Figure 1. The ceramic YA exhibited a precipitous fall in strength at 1,000°C and above, whereas YC sustained a high strength up to 1,350°C. In measurements of dynamic fatigue behavior, a high fatigue resistance was exhibited up to 900°C for YA and to 1,200°C for YC, but a precipitous fall of the relevant resistance was at 1,000°C and 1,300 °C for them, respectively. Results of measurements also proved a major difference in

internal friction between the two ceramics, and a good correlation between the internal friction and the high-temperature mechanical properties. These differences may conceivably be ascribed to differences of the grain boundary glass phases resulting from different chemical compositions.

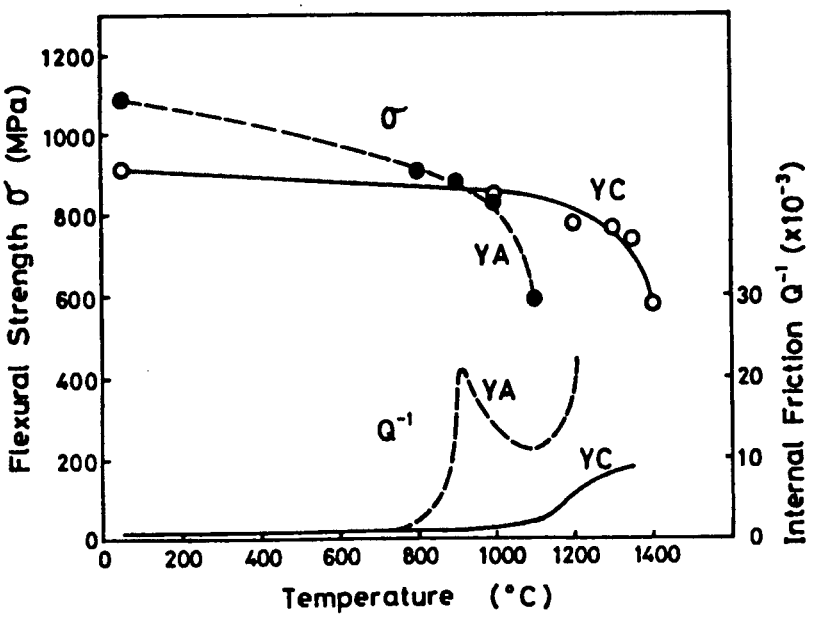

Figure 1. Plots of Temperature Vs. Strength and Internal Friction for Sintered Composites Y_2O_3–Cr_2O_3 (YC) and Y_2O_3–Al_2O_3 (YA)

Effects of Some Mullites on Thermal, Mechanical Properties of Al Titanate

906C7512 Tokyo SERAMIKKUSU KISO KAGAKU TORONKAI in Japanese 24 Jan 90 p 13

[Article by Akihiko Kawahara, Makoto Terasaki, Shuji Yoshida, and Hiroaki Katsuki, Ceramic Industry Research Institute, Saga Prefecture]

[Text] **1. Introduction**

Aluminum titanate (AT) is a ceramic that has a low thermal expansion coefficient but nevertheless exhibits low mechanical strength and tends to decompose at 900°C to about 1,300°C. In the present research, various forms of mullites were added to synthesized AT to give composite materials, and relevant thermal and mechanical properties investigated.

2. Methods and Experiment

Alumina (AES-12) of Sumitomo Chemical Co., Ltd., and Titania (TM-1) of Fuji Titanium Co., Ltd., were used as the raw materials. These were mixed equimolarly and subjected to sintering for 2 hours at 1,500°C. The product was then crushed in a pot mill made of alumina by the wet process for 50 hours to give a synthetic AT powder with an average particle diameter of about 2.6 μm. To the AT so synthesized were added any of the powders of mullite with fine particles having an average diameter of 0.5 μm, with crude particles having an average diameter of 7 μm, and with a needle form particle synthesized from New Zealand caolin (length 4~8 μm and 0.5~1 μm thick). These were added in volume ratios of 5.9, 11.6, and 21.5 percent, respectively. The wet method was used for their subsequent mixing. (For mullite powder exclusively, mixing for 12 hours with a plastic pot mill using alumina round stones was carried out.) After drying the mixture was subjected to die casting-CIP molding and to sintering for 4 hours at 1,530°C. The resultant compact was assessed for its phase structure, three-point bending strength, thermal expansion coefficient (at room temperature at about 1,000°C), bulk (relative) density, and microstructure, as was also for the rate of decomposition of AT after it had been reheated for 7 and 50 hours at 1,000°C.

3. Results

First, a quantitative analysis by means of X-ray diffraction proved that the AT having been crushed with the pot mill made of alumina after it had been synthesized at 1,500°C was contaminated by 3~4 percent corundum derived from the mill. Figure 1 presents results of measurement for the relative-density average, bending strength, and thermal expansion coefficient. The average relative density dropped when an increasing amount of mullite was added, particularly the needle form mullite since the crystals had not been dispersed satisfactorily therein and hence the compact was not compact enough. Because of the high thermal expansion coefficient of mullite, the coefficient of the compact also rose when an increasing amount of mullite was added. The coefficient of the compact also tended to rise as it grew more compact. In fine-particle and crude-particle mullite series, the bending strength was increased with an increasing amount of mullite, but, in contrast, in the needle-form mullite it tended to drop with increasing addition of mullite. AT, with no addition of mullite, decomposed fully when subjected to reheating for 50 hours at 1,000°C, but the rate of decomposition was 4~8 percent for AT with 5.9 percent of mullite added and less than 3 percent for AT with 11.6 percent or more of mullite.

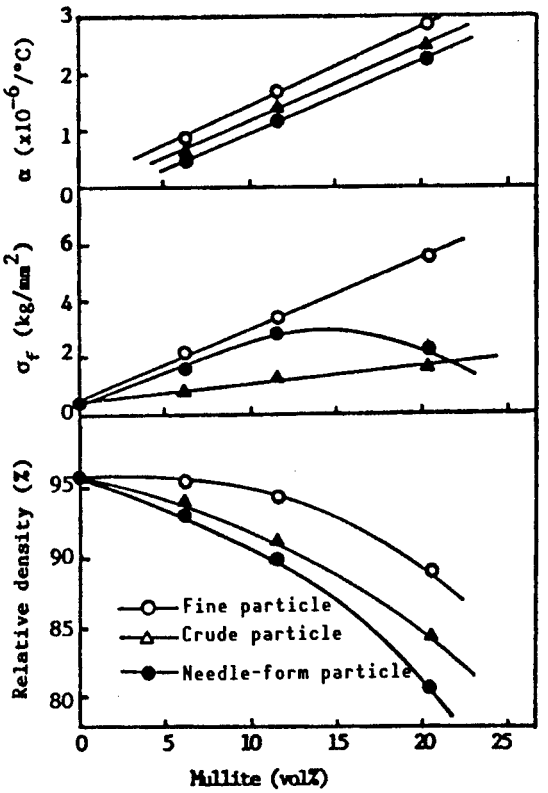

Figure 1. Changes of Thermal and Mechanical Properties for Composite of Different Forms and Sizes

Strengthening ZrO_2 Ceramics by Thermal Stress

906C7512 Tokyo SERAMIKKUSU KISO KAGAKU TORONKAI in Japanese 24 Jan 90 p 14

[Article by Hiroshi Takada, Isao Tanaka, and Kooicha Niihara, ISIR (Sanken), Osaka University, and Tetsuo Uchiyama and Shigeo Inoue, Riken Co., Ltd.]

[Text] **1. Objective of Experiment**

Al_2O_3 is a typical oxide ceramic that has a wide range of practical applications in a variety of industrial fields. However, if the ceramic is to find practical applications under harder conditions as a structural material that compares with those of the nonoxide ceramics Si_3N_4 and SiC, problems such as the following need to be resolved: 1) low strength and toughness; 2) large fall of structure at high temperature; 3) low resistance against creep; and 4) poor resistance against thermal impact. Many researchers, therefore, have been pushing ahead with solutions to these questions by such means as reinforcement of the ceramic by dispersion of TiC particles, SiC whiskers, and ZrO_2. The authors, in turn, have for several years been trying to lessen the disadvantages involved in Al_2O_3 ceramics at a stroke—with a good amount of results achieved by a method of multi-toughening, which allows the following two methods of toughening ceramics to work together without antagonistically affecting each other. One is tightening by ZrO_2, which undergoes a phase transformation induced by stress; the other is toughening by SiC whiskers, which produces crack deflection and whisker pull-out action. The objective of the present investigation is the further toughening of the ceramics of the Al_2O_3 series that have been subjected to the above multitoughening procedure by applying effectively the tensile thermal stress produced over the surface of the ceramic when it is rapidly quenched in water.

2. Method of Experiment

Fifteen percent in volume of each of ZrO_2 (TZ-2Y) and SiC whiskers was added to γ-Al_2O_3; the resultant material was subjected to mixing in acetone for more than 12 hours by means of the common ball mill method, and the mixture, after having been packed into a graphite die, was hot pressed for 1 hour at 1,500°C to about 1,600°C in a streaming argon to give a composite ceramic, Al_2O_3/15 volume percent SiC whiskers/15 volume percent ZrO_2, of high density. Disk-shaped composite ceramic pieces 50 mm in diameter and 5 mm in thickness so

produced were machined into test specimens 3 x 4 x 36 mm by lapping and cutting and were subjected to various testing. Thermal stress was applied by rapidly quenching the test specimen in water from a temperature below the critical temperature for thermal-impact destruction ΔT_c. The amount of transformation of ZrO_2 from the tetragonal to the monoclinic system was estimated by X-ray diffraction and laser-Raman methods.

3. Results and Discussion

Figure 1 presents the dependence of the strength of the test specimen on the amount of the tetragonal phase of ZrO_2 when the specimen was lapped again after it had been ground, and the one when the specimen was quenched rapidly in water. It is well known that the strength of ZrO_2 ceramics is reinforced by phase transformation produced by surface processing, but it can be seen from the figure that the strength reinforcement is further promoted by means of thermal stresses.

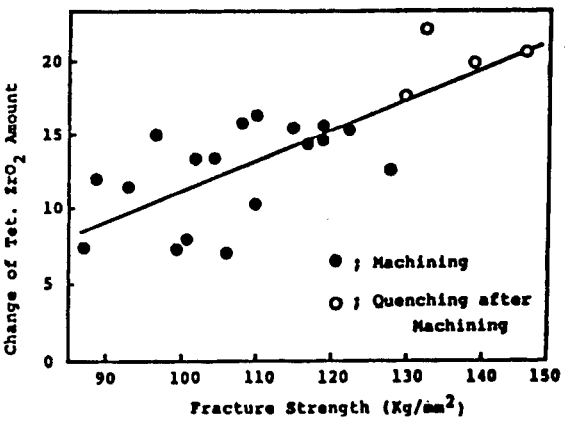

Figure 1. Change of Strength With Amount of Tetragonal ZrO_2

Microstructure, Mechanical Properties of Al_2O_3 With Dispersed SiC Particles

906C7512 Tokyo SERAMIKKUSU KISO KAGAKU TORONKAI in Japanese 24 Jan 90 p 18

[Article by Keiji Matsuhiro, NGK Insulators Co., Ltd., and Yutaka Furuse, Tokyo Electric Power Co.]

[Text] **1. Introduction**

A ceramic-ceramic composite in which alumina matrix and an SiC reinforcement material are coupled were trial manufactured by hot pressing, and the microstructure and properties of the resultant sintered compact were analyzed. It has been proved that the microstructure of the alumina matrix is controlled by the size of the SiC particle and by its amount added, and that the mechanical properties are probably dictated by many factors.

2. Experiment

The starting materials were commercially available alumina and six kinds of SiC powder of different particle characteristics. The two materials were subjected to wet-type pot mill mixing and then to drying and grading to give powder for sintering.

The powder was then hot pressed in a graphic die at a pressure of 300 kg/cm^2 and a temperature of 1,500~1,900°C under an argon atmosphere. A compact with no SiC particles involved was also prepared for comparison. The compacts were then subjected to testing for their mechanical properties, including microstructures, strength (JIS R1601 four-point bending strength), fracture toughness (SEPB method), and Young's modulus (strain gauge method).

3. Results and Discussion

The microstructure of the alumina matrix varied in large measure with the amount and particle size of SiC added. The microscopic structures of the toughened material are presented in the photographs [not reproduced]. The four-point bending test for the composite with 30 percent volume of SiC ($\bar{D}$ = 1 μm) yielded a value 816 MPa, which was higher than the value for uncoupled alumina of 562 MPa. The grain diameter of the matrix alumina, in turn, proved to be rendered particularly fine with an average diameter of

2 μm. It is conceivable that the addition of SiC fine particles rendered the crystal grain diameters of the matrix alumina finer and thus the origins of crack development finer which, in turn, led to the above rise of strength of the composite.

The fracture toughness of the composite with 30 percent volume of SiC ($\bar{D}$ = 5 μm) was 7.6 $MN/m^{3/2}$ (Photo 1 [not reproduced]) and that for the composite involving 10 percent volume of SiC (planar particle) was 7.0 $MN/m^{3/2}$ (Photo 2 [not reproduced]), which was higher than that for the uncoupled alumina of 3.8 $MN/m^{3/2}$. The microscopic picture of the above composites also presented largely different features: the composite with SiC particles having an average particle diameter of 5 μm exhibited a picture in which the SiC particles were dispersed in an alumina matrix made up of largely isodiametric 10 μm grains, and the one with addition of planar SiC particles had a crystal structure made up of planar alumina crystals of size 50 μm by 10 μm. With the pronounced effects achieved for improvement of toughness for either kind of composite above, there is the possibility of some other factors than the ones due to microscopic structure being involved in the mechanism of toughness improvement.

Effect of Undercoating on Tensile Strength of SiC-Coated Carbon Fiber

906C7512 Tokyo SERAMIKKUSU KISO KAGAKU TORONKAI in Japanese 24 Jan 90 p 19

[Article by Kuniaki Honjo, Government Industrial Research Institute, Osaka]

[Text] **1. Introduction**

Carbon fibers coated with ceramics like SiC are available for reinforcement materials. If the fiber is to have higher strength and higher toughness, it is necessary that crack propagation from the coating be blocked at the interface between the fiber and the coating. For this purpose, it is effective to reduce the interface (shearing) strength by using a film of an undercoat,[1] even though a higher interface strength is more favorable to the reinforcement agent for toughening the composite. The present report deals with the successful preparation of a fiber with both high interface strength and high fiber strength by using a carbon film containing SiC as the undercoat.

2. Method

By using chemical vapor deposition (CVD), carbon fibers were coated either with a film of an undercoat involving carbon (C) or with one of carbon and 3~5 percent by weight of SiC (C(SiC)) and, subsequently, with a film of SiC by changing the composition of the reacting gas applied. The properties of the raw material carbon fiber and the conditions for coating application are presented in Tables 1 and 2. Measurements were taken for the strength of coated carbon fibers by the monofilament method and for the interface shear strength (τ) between the SiC coating and the undercoating by the monofilament drawing method. Observation by electron beam diffraction, of the surface of the fiber exposed by fiber pullout confirmed that the surface exposed by separation was the interface between the SiC coating and the undercoating.

3. Results

Figure 1 presents a graph for interfacial shear strength τ. The value τ for the undercoat C(SiC) is 1.5~2.0 times or more larger than that for undercoat C. The difference in τ may possibly be produced by the presence of the SiC in very small amounts.

Table 1. Properties of Carbon Fibers

Fiber	Young's modulus GPa	Tensile strength MPa	Elongation to rupture %	Filament diameter μm
Torayca T300	230	3080	1.3	6.5
M30	294	3920	1.3	6.5

Table 2. Coating Conditions

Coating	T	Gas composition	Coating thickness
C	1,200°C	Propane 3, Ar 250 ml/min	.05~.1 μm
C(SiC)	1,200°C	CH_3SiCl_3 3, Ar 250 ml/min	.05~.1 μm
SiC	1,200°C	CH_3SiCl_3 3, H_2 30, Ar 250 ml/min	.1~.15 μm

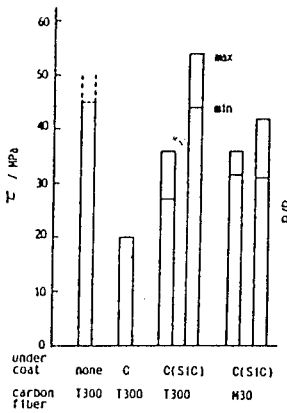

Figure 1. Interfacial Shear Strength (τ) of SiC-Coated Carbon Fibers

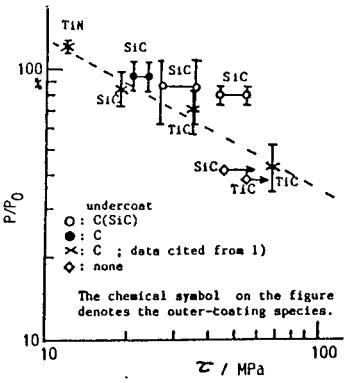

Figure 2. Relationship Between τ and Strength (Represented by relative rupture load P/P of ceramic-coated carbon fibers)

Figure 2, in turn, represents a plot in logarithmic scale of the value τ vs. the fiber strength expressed by relative rupture loads P/P_0 where P_0 denotes the strength of the fiber with no coating. The fiber with direct coating of SiC has a P/P_0 of 42 percent and elongation of 0.4 percent, a level that may conceivably allow crack development in the SiC coating. When C undercoat is added to the fiber, the relationship between τ and P/P_0 nearly corresponds to the one represented by the dotted line. In fibers with C(SiC) undercoat, however, P/P_0 has approximately a high 80 percent, whereas τ also has a high value; it is therefore conceivable that the process of crack growth at the C(SiC)-SiC interface is different from the one at the C-SiC and carbon fiber-SiC interfaces.

References

1. Honjo, K. and Shindo, A., "Composite Interfaces," ed. by H. Ishida, et al., Elsevier, 1986, p 101.

Superplasticity of Nonoxide Composites

906C7512 Tokyo SERAMIKKUSU KISO KAGAKU TORONKAI in Japanese 24 Jan 90 p 20

[Article by Fumihiro Wakai, Yasuharu Kodama, Shuji Sakaguchi, and Norimitsu Murayama, Government Industrial Research Institute, Nagoya; Kansei Izaki, Mitsubishi Gas Chemical Co., Ltd.; and Kooichi Niihara, Osaka University]

[Text] **1. Introduction**

Mechanical properties of ceramics vary in a large measure as their microscopic structures are changed. The ceramic Si_3N_4, for example, has its toughness and strength at high temperatures greatly improved by development of a long columnar crystal structure.[1] Composites involving dispersion of particles of zirconia series, in turn, exhibit superplasticity at high temperatures provided the crystal grain is very small and isodiametric. Raj, et al., predicted that Si_3N_4 must exhibit superplasticity resulting from a diffusion creep enhanced by a process of dissolution and deposition produced by way of the liquid phase of the grain boundary, but the greatest elongation reported to date remains a mere 10 percent or so. In the present research, the authors were able to demonstrate a superplastic elongation of more than 100 percent for a composite material Si_3N_4–SiC composed of very small, isodiametric grains that they produced.

2. Method of Experiment

A mixture of 70 percent by weight of Si_3N_4 and 30 percent by weight of SiC in fine powder prepared by the vapor phase reaction method and having 6 percent by weight of Y_2O_3 and 2 percent by weight of Al_2O_3 added as sintering promoters was subjected to hot pressing. The resultant composite had a density of 3.28 g/cm^3 (TD: 9.9 percent up), a fracture toughness of 5.5 $MN/m^{2/3}$, and a four-point bending strength at room temperature of 820 MPa. The relevant tensile test was carried out under a 1-atm. nitrogen atmosphere at 1,650°C and at a constant crosshead speed.

3. Results

Test specimens of the composite Si_3N_4–SiC before and after deformation are compared in Figure 1 [not reproduced]. A superplastic elongation of 105 percent was obtained from an initial strain rate of about 8 x $10^{-5}s^{-1}$, but no pronounced elongation was seen in both cases where the strain rate is too high and where it is too low. Figure 2 [not reproduced] presents a scanning electron microscope (SEM) photograph of the fractured surface; the composite consisted of isodiametric particles of a size around 0.2 μm. A strain hardening was observed in true stress vs. true strain curve. Where the specimen was deformed at a low strain rate, and hence exposed to high temperatures for long hours, the color of its surface turned whitish and cracks directed vertically to the axis of the stress developed, which has proved to be the result of decomposition of Si_3N_4 at high temperatures.

References

1. Izaki, K., Hakkei, K., Ando, K., Kawakami, T., and Niihara, K., "Ultrastructure Processing of Advanced Ceramics," John Wiley & Sons, 1988, pp 891–900.

Superplasticity of Hydroxyapatite

906C7512 Tokyo SERAMIKKUSU KISO KAGAKU TORONKAI in Japanese 24 Jan 90 p 21

[Article by Fumihiro Wakai, Yasuharu Kodama, Shuuji Sakaguchi, and Norimitsu Murayama, Government Industrial Research Institute, Nagoya, and Tooru Nonami, TDK Co., Ltd.]

[Text] **1. Introduction**

Hydroxyapatite, $Ca_{10}(PO_4)_6(OH)_2$ (HAp for short), is a material of superior biocompatibility. Since Jarcho, et al., demonstrated that the material, when processed by the wet process and subjected to sintering under normal pressure, afforded a compact having a high density and fine particle diameters, there have been developed polycrystals with still finer particle diameters by means of hot pressing and HIP. Although zirconia of the fluorite structure has proved to exhibit fine-crystal superplasticity, no reports have to date been made on the high-temperature transformation of HAp, despite its complex crystal structure involving the OH group. In the present research, the authors were able to demonstrate in HAp the fine-crystal superplasticity of a type different from that for zirconia.

2. Method for Experiment

A HAp powder prepared by the wet process (Ca/P = 1.67) was subjected to sintering in air (1,050°C, 2 hours) and then to HIP (203 MPa, 1,000°C, 2 hours) to give a sintered compact with compact consistency and transparency to light (H: HIPed material; TD: 99.9 percent; grain diameter: 0.67 μm). The grain diameter was defined as being 1.776 times the relevant length of the section. The deformation behavior of the specimen was studied by carrying out high-temperature tensile tests in air, and those specimens sintered under normal pressure (N: grain diameter 1.07 μm, white) were also subjected to the same test to run the control.

3. Results

Figure 1 presents a comparison of the HIPed test specimen before deformation by the tensile test with the one after it. The specimen that exhibited 130 percent or more superplastic elongation had a uniform deformation in the gauge

section of the specimen, which, following the deformation, lost its transparency to light and turned opaque. Figure 2 represents a stress vs strain curve of the test, which displays a strain hardening, a phenomenon in which stress increases with increasing deformation. The intersection of the linear portion of the stress vs. strain curve and the stress axis was defined as surrender stress, σ_0. Assuming that the following relationship exists between the strain rate and the surrender stress

$$\epsilon = A\ \sigma_0^n/d^p\ \exp\ (-Q/RT) \qquad (1)$$

n was calculated as being 4~5 and Q/n as 169 kJ/mol. Observation by scanning electron microscope (SEM) of the microstructure after deformation showed a pronounced grain growth in HIPed specimens. The proportion of intragrain strain in the total strain, as calculated on the basis of the aspect ratio of the grain, was 20 percent and the strain thus was assumed to have been produced largely by grain boundary slip. Specimens sintered under normal pressure also exhibited strain hardening, but their rupture elongation was less than 35 percent.

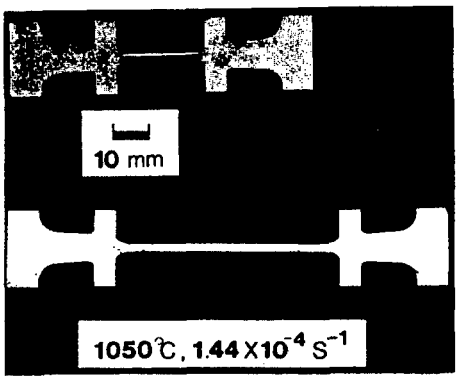

Figure 1. Superplasticity of HAp

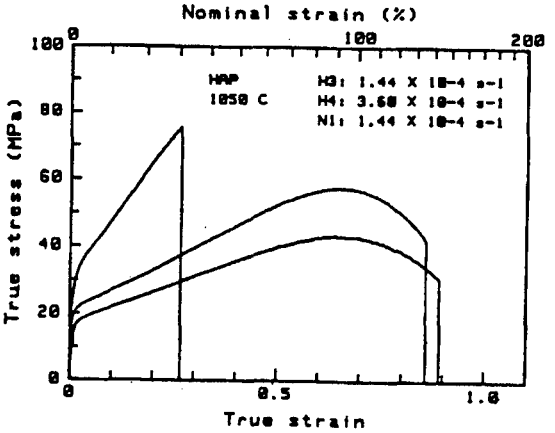

Figure 2. Stress-Strain Curves of HAp at 1,050°C

Fabrication of TiB_2-Ni Functionally Gradient Materials by Gas-Pressure Combustion Sintering

906C7512 Tokyo SERAMIKKUSU KISO KAGAKU TORONKAI in Japanese 24 Jan 90 p 30

[Article by Toshikazu Takahura, Isao Tanaka, and Yoshinari Miyamoto, Sanken (ISIR), Osaka University, and Osamu Yamada, Osaka Industrial University]

[Text] **1. Introduction**

The authors had previously produced composite materials of TiB_2–Ni series by means of gas pressure combustion sintering and had carried out an evaluation of relevant combustion characteristics and control of the microstructure of the product. In the present investigation, based on the above result, functionally gradient materials of the TiB_2–Ni series have been prepared, and microstructure and mechanical properties of the product evaluated.

2. Method of Experiment

The powders of Ti, B, Ni, and TiB_2 in given proportions were subjected to wet mixing for 24 hours and then to drying in vacuum. The mixed powders were subsequently laminated and molded into a cylinder, diameter 13 mm, such that each layer had a thickness of 2~4 mm, and the resulting product was sealed into a vacuum glass capsule. The capsule, together with the ignition agent of Ti and C, was packed into a carbon crucible and installed in an HIP machine. The igniting agent was then fired under a given condition, that is, at a temperature of 700°C and a pressure of 100 MPa, such that the heat generated induced a synthetic reaction of the material in the capsule, which was completed simultaneously with the sintering. After the density, X-ray diffraction, etc., of the sintered compact so produced had been evaluated, its surface was lapped into mirror face and its microstructure was observed by scanning electron microscope (SEM).

3. Results and Discussion

Figure 1 represents a plot of the relative density vs. the amount of Ni added. As can be seen, the increase in density is limited to 96 percent where Ti is not present in excess of 10 percent or more by weight, but otherwise the density increases near to the theoretical value and corresponding compactness.

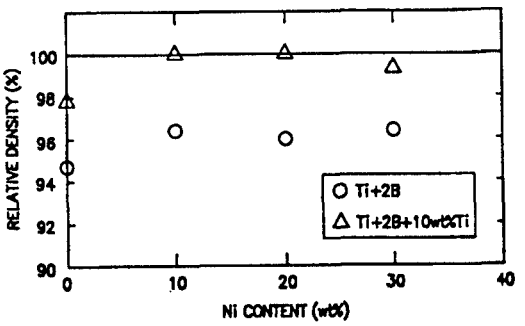

Figure 1. Relative Density of TiB_2–Ni Based Composites

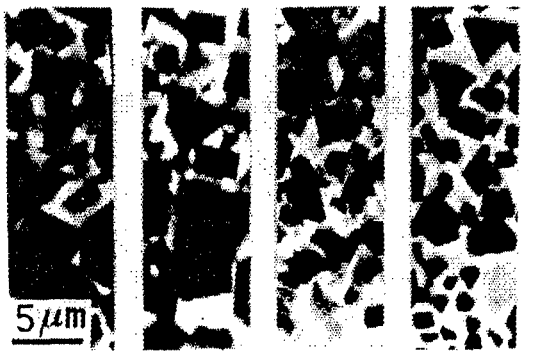

Figure 2. SEM Image of Polished TiB_2–Ni Gradient Material

This may conceivably be ascribed largely to the vaporization of B_2O_3 in the material powder being blocked by the presence in excess of Ti. For this reason, a material powder involving Ti in excess by 10 weight percent and with Ni added (composition denoted by Δ in the figure) was laminated stepwise as above and subjected to gas pressure combustion sintering. A photograph of the lapped surface of the compact so produced is presented in Figure 2, which shows that the compact is free from any pores and has almost perfect compactness in consistency, like compacts of single component materials, and which also shows that there are no definite borderlines between each adjoining two layers despite the stepwise lamination, namely, that the composition varies gradually. The diameter of the grain of TiB falls gradually with increasing amounts of Ni (from left to right in the figure), which may imply a corresponding fall of the relevant combustion temperature.

Some Properties of SiC-C Functionally Gradient Material Prepared by CVD

906C7512 Tokyo SERAMIKKUSU KISO KAGAKU TORONKAI in Japanese 24 Jan 90 p 31

[Article by Makoto Sasaki and Toshio Hirai, IMR (Kinken), Tohoku University; Toshiyuki Hashida and Hideaki Takahashi, Department of Technology, Tohoku University; and Junichi Teraki and Tooru Hirano, CAE Center of Daikin Industries Co., Ltd.]

[Text] **1. Objective**

Materials available in extremely dangerous environments, such as in space and aircraft operations, have recently been in demand. One such example is a composite in which the composition gradually changes from one side of a body to the other, and hence the relevant functions similarly change, and which is referred to as a functionally gradient material, FGM. The authors carried out synthesis by chemical vapor deposition (CVD) of an SiC/C-FGM--a material in which the composition varies from SiC to C and has a high resistance to oxidation and a high-temperature strength on the one side but has a low value for Young's modulus and is amenable to fabrication on the other--and studied its respectively to thermal impact and its heat insulation characteristics.

2. Method

The material used consisted largely of $SiCl_4$, CH_4, and H_2, with the container of $SiCl_4$ being kept at 20°C and H_2 used as the carrier. The amount of flow of the material gas was varied continuously by using a sequencer. The synthesis was carried out for 9 ks at temperatures of 1,673 K and 1,773 K under a total pressure of 1.3 kPa.

The material thus produced was studied for its resistance to thermal impact by use of CO_2 laser and for its heat-insulation capacity and resistance to thermal fatigue by use of a high-temperature gradient testing apparatus that provided a xenon arc lamp for heating and liquid nitrogen for forced cooling.

3. Results

The specimens produced at 1,773 K and 1,673 K had compositions closest to the one at which the stress produced therein is minimized. The surface of the CVD deposition exhibited a pebble-like structure unique to that of the SiC subjected to synthesis under the same conditions. Observations by scanning electron microscope (SEM) proved that materials with a gradual change of composition from C to SiC were produced, although the film had a somewhat porous structure near the center.

Testing for resistance to thermal impact were conducted for SiC·NFGM, (non-FGM), SiC+C·NFGM, and SiC/C·FGM with a laser-heat thermal impact tester, which proved that both NFGM and FGM suffered no cracks by repeated heating with laser, that is, there was no significant difference in relevant reaction between the two and no acoustic emission (AE) signals were detected except at the noise level for both SiC and SiC/C·FGM and, hence, resistance of both to rupture in forced heating.

Heating involved a temperature gradient in which the front surface for the specimen was at 1,700~1,150 K and the rear surface at 1,200~900 K was applied 40 times in vacuum; the result showed development of cracks in the SiC film at the interface between the SiC film and the substrate for the SiC·NFGM specimen, which may conceivably be ascribed to thermal fatigue due to repeated heating. SiC/C·FGM, in contrast, exhibited fine results with no changes noted. The film of the specimen of SiC·NFGM, formed in thickness of 0.4 mm on a graphite substrate having a thickness of 10 mm, in turn, showed a heat insulation capacity of 300 K at a thermal flow of about 0.7 $MW \cdot m^{-2}$, whereas SiC·FGM under the same conditions displayed a superior result with a heat insulation of 400 K, which was proved to be the result of high heat/insulation temperature within the FGM layers than within the NFGM layers.

Acknowledgement: The authors express their gratitude to the Kakuta Branch of Kogiken (Aerospace Technology Laboratory) for extended cooperation in the high-temperature gradient test.

Characteristics of Carbon Fiber Reinforced SiC Composite Fabricated Using Polysilazane

906C7512 Tokyo SERAMIKKUSU KISO KAGAKU TORONKAI in Japanese 24 Jan 90 p 32

[Article by Kikuo Nakano and Akira Kamiya, Government Industrial Research Institute, Nagoya; Hiroshi Okuda, Fuji Research Institute, Tokai Carbon Co., Ltd.; and Tadayuki Mitani and Yoshihiro Abe, Nagoya Institute of Technology]

[Text] **1. Introduction**

Many attempts have been made in recent years to make tougher SiC, a prospective high-temperature material, and the use of carbon fibers represents the most promising of all for that purpose. The authors have been trying to produce SiC composites by using slurry impregnation, which involves organic polymers as the precursor and which may possibly allow high yields and low costs.[1] This report deals with an investigation of properties of an SiC composite ceramic that is reinforced with carbon fibers and is prepared by using polysilazane resin.

2. Method of Experiment

The materials used comprise carbon fibers (PAN type or high-elongation type, Toho Rayon Co., Ltd., ST-3; and pitch type or high-modulus of elasticity type, PETOCA, HM-50, HM-60) for the reinforcement material, silicon carbide powder (Herma C. Stark, β-SiC, B-20, 0.6 μm) for the filler, AlB for the sintering promoter, and polysilazane (Chisso Co., Ltd., NCP 200) for the resin. The prepreg of the composite was prepared from these materials by filament winding and the compact was from the prepreg through the dewaxing and hot pressing processes (argon, 1,750~1,850°C) (unidirectional fiber reinforcement). The specimen so obtained was subjected to evaluation of its sintering characteristic, observation of its microstructure, and measurement of its bending strength (three-point bending strength, normal temperature, normal to the running direction of the fiber), and fracture toughness (SENB method).

3. Results

Table 1 presents the pore ratio for the SiC composite ceramics reinforced with carbon fibers. In all types of the SiC composite, the ratio falls and the

strength rises with increasing combustion temperature. Also, the specimens reinforced with the pitch type fibers exhibit higher values of strength than those reinforced with the PAN type, which may possibly be attributed largely to the reaction with the matrix of carbon fibers being substantially lower for the pitch type than for the PAN type. The reaction with the matrix, nevertheless, increases substantially even for the pitch type fibers when the sintering temperature reaches 1,850°C (Figure 1). Carbon-fiber reinforced SiC composite ceramics involving use of polysilazane as the resin tended to have high open-pore ratios and low strength in comparison with those in which polystyrene was used as the resin. Results of the bending test of the specimen, in turn, indicated that cracks propagate both along the line of separation at the interface between the fiber and the matrix and in the direction vertical to that of the running fiber (Figure 2).

Table 1. Mechanical Properties of Fiber-Reinforced Composite Ceramics

Type of fiber	Sintering temperature (°C)	Rate of open pores (%)	Bending strength (MPa)	Klc (MPa$\sqrt{m}$)
HM-50	1,750	16.7	194.9	4.6
	1,800	9.7	203.2	6.4
HM-60	1,750	15.3	78.2	2.1
	1,850	14.2	127.2	5.1
ST-3	1,800	11.5	30.1	2.1

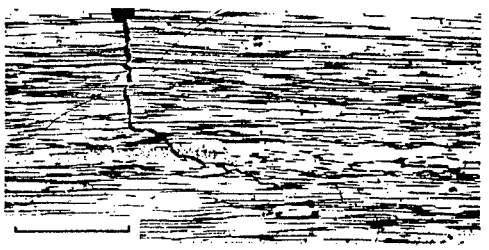

Figure 1. Reflection Electron Beam Picture of Composite Ceramic SiC Reinforced With Carbon Fiber (Pitch type of HM-50, sintered at 1,850°C, scale 10 μm)

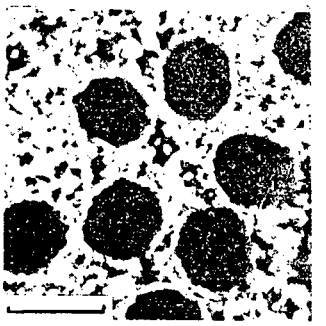

Figure 2. Growth of Cracks in Vicinity of Notch (Pitch type HM-60, sintered at 1,850°C, scale 1 mm)

Results of X-ray diffraction tests on the specimens prepared in the present experiment showed hardly any diffraction lines other than the one for the β-SiC phase.

References

1. Nakajima, K., et al., Preliminary Manuscript for Lectures at the 1989 Annual Meeting of the Japan Ceramic Institute, 2E33.

Pressureless Sintering of SiC-Platelet Dispersed Si_3N_4 Composites

906C7512 Tokyo SERAMIKKUSU KISO KAGAKU TORONKAI in Japanese 24 Jan 90 p 33

[Article by Tatsuo Noma, Tokyo Institute of Technology, and Michael J. Hoffmann and Guenter Petzow, Max Planck Institute]

[Text] **1. Introduction**

Dispersion in ceramics of whiskers and other particles with an anisotropy in shape allows improvement of fracture toughness by virtue of their crack-deflection effects, etc. It was expected that dispersion of platelet particles therein will bring about similar effects as shown in Figure 1. Therefore, in the present investigation, the authors tried to produce a more compact composite largely by means of pressureless sintering of the material Si_3N_4 with SiC platelets added in dispersion. In addition, the composite Si_3N_4 with SiC whiskers added in dispersion[1] was compared with the above product.

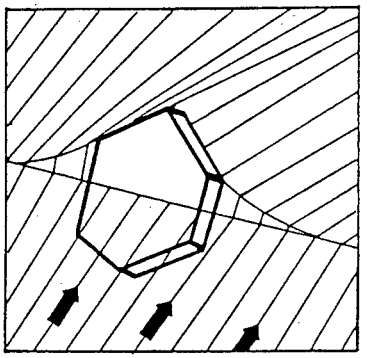

Figure 1. Crack Deflection by a Platelet

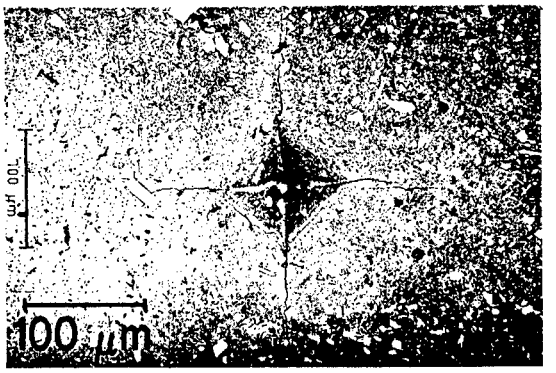

Figure 2. Crack Propagation in a Composite

2. Method of Experiment

The starting materials used were SiC platelets with an average diameter of 17 μm and an average thickness of 3 μm (made by AMI Corp.) and Si_3N_4 powder (LC-12S, made by H.C. Stark Corp.) with Al_2O_3 and Y_2O_3 added as sintering promoters. Following a CIP molding, the material was subjected to a

pressureless sintering under a nitrogen atmosphere and at a temperature of either 1,850°C or 1,900°C, and, for part of it, further to an HIP treatment at 2,000°C and 100 MPa under a nitrogen atmosphere. Subsequently, by varying the amount of SiC, those of sintering promoters, and temperature profiles in pressureless sintering, their effects on the compactness and microstructure of the specimens were studied.

3. Results

Figure 2 presents a picture of a crack developed after driving a Vickers diamond pyramid onto the surface of a specimen with a composition involving 15 percent in volume of SiC and 10 percent by weight of the sintering promoters (made exclusively by pressureless sintering) and with a relative density of 96.7 percent. Cracks were deflected by the platelet particles, with the maximum effect of crack deflection displayed particularly by platelets with a diameter of about 10 μm. Particles with a platelet diameter smaller than that value often showed a picture of cracks penetrating through platelets, and those with a platelet diameter greater than that value separated at the interface.

The composite, compared with those involving whiskers in dispersion, has the advantage that the amount of sintering promoters necessary may be reduced and that the platelets for dispersion are not subject to aggregation during mixing; however, it also suffers such disadvantages as cracks developing at the interface in cases where compactness of the specimen is not satisfactory and that grinding and lapping of the specimen are difficult. Fracture toughness and other mechanical properties and microstructures in greater detail are to be reported additionally in the coming lecture.

References

1. Hoffman, M.J., Dr.rer.nat., Dissertation, Uni. Stuttgart, 1989.

Preparation of SiC-Si_3N_4 Composite Powder From Si_3N_4 Mixture by YAG Laser

906C7512 Tokyo SERAMIKKUSU KISO KAGAKU TORONKAI in Japanese 24 Jan 90 p 34

[Article by Takeshi Okutani, Yoshinori Nakata, Masaaki Suzuki, and Munehiro Yamaguchi, GIDLE (Government Industrial Research Institute, Hokkaido); Junich Watanabe, Suzuki Shoko Co., Ltd.; Masanobu Kikuchi, IMC; and Tatsuya Yoshii, Denka Co., Ltd.]

[Text] **1. Introduction**

In an earlier report, the authors presented a method of preparing SiC from a mixture of SiO_2-C by irradiating the material with a YAG laser with its frequency range covering the infrared region.[1] The present report deals with preparation of a mixture of powder made up of SiC involving a superior high-temperature strength and Si_3N_4 displaying fine resistance against thermal impact by means of irradiation with the same beam.

2. [Method of Experiment]

The materials used consisted of Si_3N_4 powder (made by Denka; SN-B with β-type as the major component, SN-5 with α-type as the major component, SN-9 containing α- and β-types in approximately equal amount; -325 mesh) and, as the C source, petroleum cokes (crushed with planetary ball mill (PBM) for 5 minutes; water, ash, and volatile component all at 0.1 percent, fixed carbon at 99.3 percent, and C at 98.6 percent). The two components were weighed and mixed for 10 minutes with the PBM in the molar ratio of C to Si_3N_4 of 1~12. The apparatus used is shown in Figure 1. The YAG laser oscillation unit was model 96200 made by Laser Application Inc. (cw, maximal output 300 W). The specimen was introduced into a transparent quartz tube (8 mm in internal diameter and 30 cm in length) such that it occupies about one-half of the volume of the tube. The tube, set horizontally, was rotated at 4.44 rpm and shifted lengthwise at 5 mm/minute with N_2 or CH_4 gases being passed at 100 mℓ/minute through the tube. The specimen in the tube was irradiated with an 8-mm diameter, 60~280 W laser beam to induce the relevant reaction at a temperature of 1,500~2,200°C. The powder thus produced was allowed to stand for 30 minutes under an air flow at 750°C to eliminate free carbon and then subjected to X-ray analysis; chemical analysis of Si, C, N, and O; scanning electron microscope (SEM); and SAD.

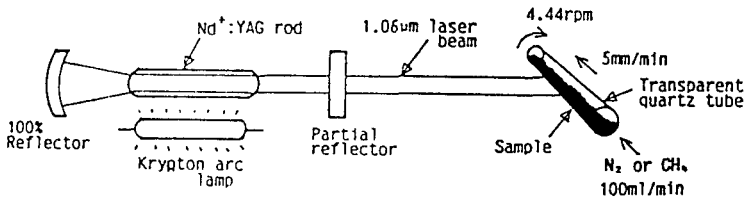

Figure 1. Schematic Diagram of a YAG Laser Irradiation Apparatus

3. [Results]

Results of irradiation of a mixture of Si_3N_4(SN-B)-C (molar ratio 1~12) with a YAG-laser beam having an output of 60~280 W follows. By varying the YAG-laser output and the ratio of C to Si_3N_4, 40~90 percent of Si_3N_4 was subjected to the relevant conversion. X-ray diffraction of the powder thus produced showed that the powder produced by irradiation under nitrogen atmosphere was β SiC and that Si was also detectable in the product, providing the material mixture had a C-to-Si_3N_4 ratio below 6.0, with the amount of Si increasing as the ratio decreased. In the case of irradiation under CH_4 atmosphere, however, no Si was detectable, the product being exclusively β SiC. SEM observation of the powder so produced showed that, with irradiation under nitrogen atmosphere, the β SiC was whisker-like in form, with the particle form increasing in number as the laser output was increased and as the C-to-Si_3N_4 ratio was increased, and that these whiskers and particles came together into secondary spherical particles 100~200 μm in diameter. With irradiation under CH_4 atmosphere, however, no whiskers were observed, but particles of 1~5 μm in diameter attached together into secondary spherical particles of 100 μm in diameter. The mechanism of formation of SiC from the mixture of Si_3N_4 and C may conceivably involve first heating of C by the laser and next of Si_3N_4 by either convection or transfer of heat, with subsequent decomposition of the compound into Si and N_2 followed by reaction of resulting Si with C to give SiC. With the Si so produced having a melting point of 1,414°C, a rise of temperature of the specimen by laser irradiation up to 1,500~2,200°C brings the Si into the fused state, a factor that may conceivably influence the shape of the particles yielded. Si_3N_4 containing some α Si_3N_4 was also studied.

References

1. Okutani, et al., CERAMIC ARTICLE JOURNAL, Vol 97, 1989, pp 1537-1542.

Oxidation Behavior of Oxide/SiC-Whisker Composites

906C7512 Tokyo SERAMIKKUSU KISO KAGAKU TORONKAI in Japanese 24 Jan 90 p 36

[Article by Satoshi Iio, Hitoshi Yokoi, Masakazu Watanabe, and Yasushi Matsuo, NGK Spark Plug Co., Ltd.]

[Text] **1. Introduction**

In recent years, research has been widely conducted for toughening composites by dispersing SiC whiskers (SiC_w) in a ceramic matrix and, in this connection, the importance of antioxidation characteristics of the relevant ceramics has been suggested in terms of their application in high-temperature structural materials. In this investigation, ceramics reinforced with SiC whiskers and involving a variety of oxides as the matrix were prepared, and relevant oxidation behaviors investigated.

2. Experiment

Twenty percent in volume of SiC_w was added to each of the powders of Al_2O_3, $Al_6Si_2O_{13}$(mullite), 3Y-PSZ, and $ZrSiO_4$, and subjected to wet mixing with the ball mill, then to drying and to pelletizing to give material powders. The powders were next subjected to hot pressing for from one-half to 1 hour at 1,500~1,850°C and at 200~400 kg/cm^2 to give a compact. Oxidation tests were performed on these composite materials and, for control, on the compound SiC_w at 800~1,300°C for 200 hours.

3. Results and Discussion

Figure 1 presents the relationship of the temperature at which the composite materials and SiC_w were oxidized for 100 hours to the rate of conversion from SiC_w to SiO_2. The resistance against oxidation of the materials decreased in the order $Al_6Si_2O_{13}$ > Al_2O_3 > $ZrSiO_4$ > 3Y-PSZ. It was notable that, because of its high oxygen diffusion coefficient, the 3Y-PSZ matrix had the SiC_w oxidized to an extent equal to that for the noncomposite SiC_w. X-ray diffraction tests also showed that, where Al_2O_3 or 3Y-PSZ was used as the matrix, $Al_6Si_2O_{13}$ and $ZrSiO_4$ were detectable, which may conceivably have been precipitated by a reaction of the matrix with SiO_2 which, in turn, was derived from SiC by oxidation. It may be concluded from the above that oxidation of SiC_w in oxide/

SiC_w composite materials are dictated by the oxygen diffusion coefficient in the matrix and a reaction of the matrix with SiO_2 and that, in designing a high-temperature structural material from among these composites, selection of an oxide that has low oxygen diffusion coefficient and that is reluctant to react to SiO_2 is to be more favored.

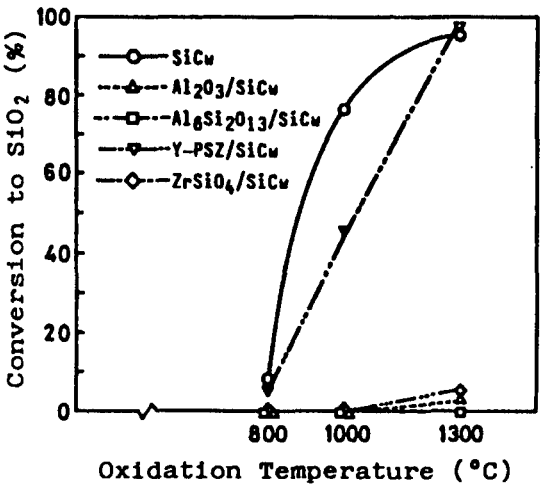

Figure 1. Oxidation Characteristics of Composite SiC_w and SiC_w Grains in Matrixes of Different Oxide Ceramics

Preparation of TiC-C Composite by Chemical Vapor Deposition

906C7512 Tokyo SERAMIKKUSU KISO KAGAKU TORONKAI in Japanese 24 Jan 90 p 37

[Article by Hiroyuki Suzuki, Makoto Sasaki, and Toshio Hirai, Institute for Material Research, Tohoku University]

[Text] **1. Introduction**

Titanium carbide, TiC, represents a material of excellent heat resistance; carbon, C, represents one with good thermal impact resistance. It is reasonable, therefore, to expect that a material with a composition that varies continuously in content of SiC and C—that is, a functionally gradient material (FGM)—might be a material for use under extremely severe temperature conditions. With the view to materializing this FGM, TiC-C composites involving varying contents of TiC and C were prepared by means of chemical vapor deposition (CVD); the intent was to elucidate the relationship between conditions for the synthesis and the chemical composition of the deposit and the relationship between the chemical composition and the properties of the composites.

2. Experiment

By using a CVD oven of the hot wall type, TiC-C composite materials were synthesized from a gaseous material consisting of $TiCl_4$, SH_4, and H2 on a graphite substrate at a temperature (T_{dep}) of 1,573~1,773 K and a total oven pressure (P_{tot}) of 1.3 kPa. By varying the molar ratio of the material gases from 2.0 to 65.0, composites with a variety of chemical compositions were yielded. After having separated the film from the substrate, measurements were taken for the density, lattice constant, chemical composition, etc.

3. Results

Figure 1 presents a plot of the molar ratio of the input gases vs. the chemical composition of the composite produced. By varying the molar ratio of the input gases under the conditions of T_{dep} = 1,773 K and P_{tot} = 1.3 kPa, composites with their chemical-composition ratios in the range of 02.~0.55 were afforded. Figure 2 represents the relationship of the lattice parameter and the density of the product to the chemical composition analyzed.

The lattice parameter had a value approximately corresponding to that of $TiC_{1.0}$. It is conceivable, therefore, that the product is made up of two phases, the TiC phase and the C phase. The density, in turn, fell linearly from 4.8 down to 3.0 with increasing C content.

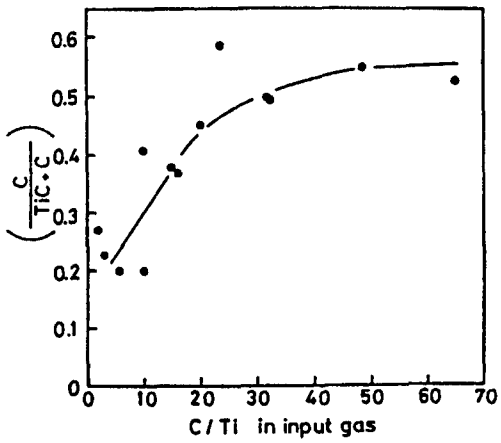

Figure 1. Relationship Between the Compositions Estimated by Chemical Analysis and the Molar Ratio of the Material Gases

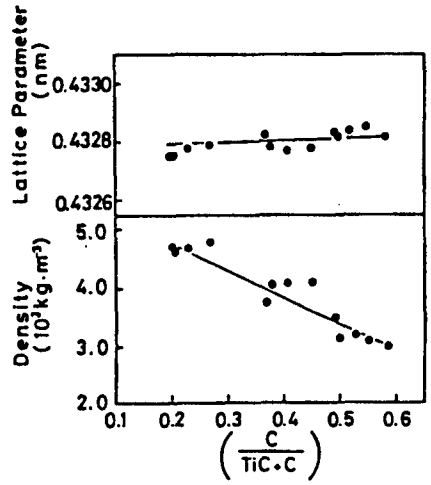

Figure 2. Dependence of Compositions Yielded by Chemical Analysis on the Lattice Parameters and the Density

Preparation of Ceramic Composite TiC/TiB_2 Having High Toughness

906C7512 Tokyo SERAMIKKUSU KISO KAGAKU TORONKAI in Japanese 24 Jan 90 p 38

[Article by Akira Kamiya and Kikuo Nakano, Government Industrial Research Institute, Nagoya, and Hiroshi Okuda, Fuji Research Institute, Tokai Carbon Co., Ltd.]

[Text] **1. Introduction**

With the view to increasing the K_{IC} of ceramics, methods of dispersing whiskers and particles in the matrix or compositing carbon fibers in the matrix, among others, have been selected and executed such that relevant structures can be made more complex and fracture energies increased. Although dispersion of particles is the cheapest and the simplest means, its effects in improving strength and toughness do not generally compare with the ones by fiber reinforcement. If dispersion of particles can afford toughening of ceramics as effectively as does whisker dispersion, practical application of ceramics would undoubtedly be enhanced enormously. It sometimes happens that sintering of a mixture of different kinds of ceramics produces a chemical reaction leading to a complex structure of the compact produced, and it is reasonable to expect that, by utilizing such a reaction, a ceramic with higher fracture energies may be produced than the one made by simple particle dispersion. The authors have to date engaged in research of the composite TiC reinforced with SiC whiskers. This report, therefore, deals with an investigation of the possibility of ceramics with enhanced toughness referred to above by using TiC as the matrix, and with a comparison of the product ceramics with those reinforced by whiskers.

2. Experiments and Results

The reaction given by

$$2TiC + B_4C = 2TiB_2 + 3C$$

is an exothermal one and, hence, sintering of a mixture of TiC and B_4C leads to the formation of the composite ceramic TiC/TiB_2. To TiC (Japan New Metal Co., Ltd.) TiC-M was added 5.10 and 20 percent by weight of B_4C (Kyouritsu Refractory Co., Ltd.: B_4C-H); the mixture was subjected to hot pressing under

argon atmosphere to give a compact. X-ray diffractometry of the compact showed no diffraction lines for B_4C but those for TiC and TiB_2 and, additionally, a line at $2\theta = 26.4°$ which may possibly indicate the presence of carbon. Figure 1 presents a reflected electron beam picture by EPMA of the compact produced by hot pressing for 1 hour at 1,900°C of a material having 10 percent B_4C: The bright crystals represent TiC and the surrounding gray phase TiB_2, while the black part represents carbon and air pores. The bending strength reached 749 MPa maximally (B_4C, 10 weight percent; hot pressing at 1,900°C for 1 hour). Figure 2 presents a stress vs. strain plot for the bending test. From point a to point b in the figure, the plotted line shifts from linearity, indicating that a multiple fracture has occurred. Figure 3 gives an scanning electron microscope (SEM) photograph of a fractured surface as viewed from the side. As can be seen, the crack runs vertically to the plane of fracture.

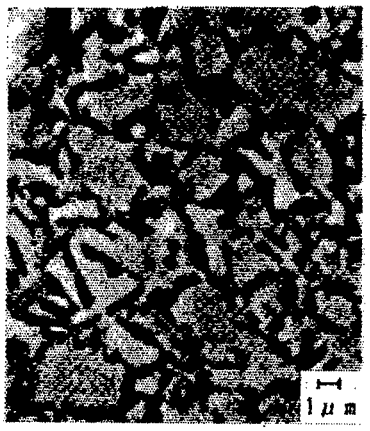

Figure 1. EPMA Reflection-Electron Beam Picture

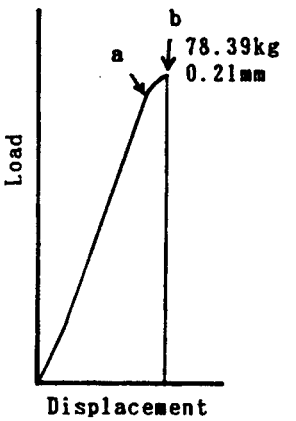

Figure 2. Plot of Stress Vs. Strain in a Bending Test

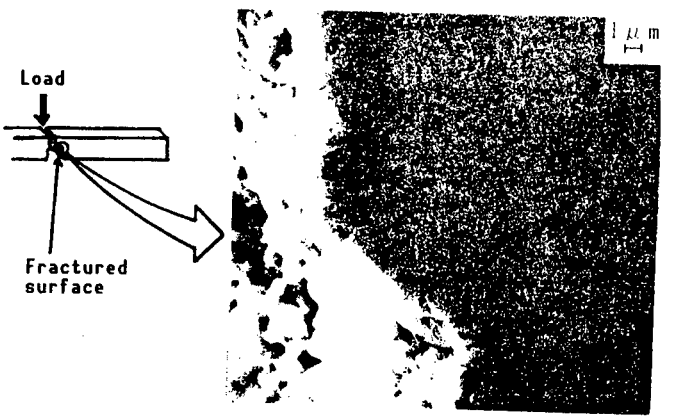

Figure 3. SEM Picture of the Fractured Surface

Preparation of Alumina-Particulate Composites by Metal Infiltration Methods

906C7512 Tokyo SERAMIKKUSU KISO KAGAKU TORONKAI in Japanese 24 Jan 90 p 39

[Article by Junichi Hojou, Osamu Sagawa, and Akio Kato, Faculty of Engineering, Kyushu University]

[Text] **1. Introduction**

Application of metal-coated ceramic particles prepared by the pelletizing-coating method produces a sintered compact in which ceramic particles are uniformly dispersed in the metal matrix.[1] This report deals with research on the manufacture of a composite using the metal infiltration method for infiltrating Ni-coated Al_2O_3 particles into porous compacts.

2. Experiment

By using the pelletizing method, 45 μm or 250 μm Al_2O_3 particles were coated with 1 μm W-powder and, following thermal treatment at 1,500°C under H_2, the product was again coated with 5 μm Ni powder. The Ni coated particles were used after having been treated thermally at 1,000°C or without the treatment. The powders so prepared were subjected to molding under pressure and sintered at 1,400°C and under H_2 for 4 hours. Ni or Cu pellets were then placed over the porous sintered compact produced, and the metal infiltration was carried out at 1,460°C for Ni and at 1,100°C for Cu.

3. Results and Discussion

The relative densities of the sintered compacts and the metal-infiltrated compacts, both involving Ni-coated particles, are presented in Table 1. The density of the sintered compact involving Al_2O_3 of diameter 250 μm does not differ significantly from that of the molded body, indicating that a compacting process has not materialized. The reason is that Al_2O_3 in the molded compact has a skeletal structure formed by cross-linkage of the Al_2O_3 particles and, hence, no contraction or compacting process. In compacts involving Al_2O_3 of diameter 45 μm, the compacting process progressed appreciably, but no sintered compact of high density was obtained. The tungsten intermediate layer in the coating of the particle acts to enhance the bonding strength and wetting action between the Ni and Al_2O_3; liquid-phase sintering at temperatures

even above the melting point of Ni, however, did not allow an increase in the density of the compact. Finally, the sintered compact of the Ni-coated particles were subjected to metal infiltration with Ni or Cu, which led to a rise in the relative density of the compact up to above 95 percent. Although wetting action between fused metals and Al_2O_3 is poor, allowing no metal infiltration at all, the sintered compact of metal-coated particles may have the metal layer over the surface of the particles letting fused metals into the pore and thus the process of Ni or Cu infiltration going on with ease. Figure 1 is an SEM photograph of a cross section of the Cu-infiltrated compact, showing that Al_2O_3, Ni, and Cu constitute a multiple-phase structure with Al_2O_3 in intimate contact with the metal phases.

Table 1. Relative Density of Composites With Dispersed Al_2O_3 Particles

Specimen	Al_2O_3: 250 μm			Al_2O_3: 45 μm		
	Al_2O_3: W:Ni:Cu (Vol%)	Relative density (%)		Al_2O_3: W:Ni (Vol%)	Relative density (%)	
		Molded body	Sintered compact		Molded body	Sintered compact
Sintered compact	50:10:40	74	74	52:18:30	75	83
Sintered compact (HT)	50:10:40	65	66	52:18:30	66	71
Ni infiltrated body	36:8:56	65	97	37:12:51	71	99
Cu infiltrated body	33:7:27:33	65	95	—	—	—

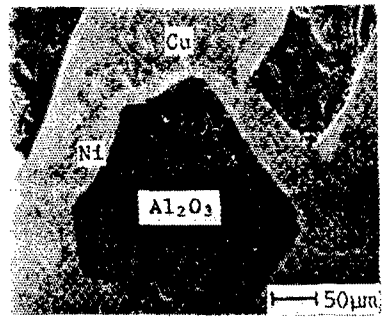

Figure 1. Cu Infiltrated Body

References

1. Hojou, et al., POWDER AND POWDER METALLURGY,Vol 36, 1989, pp 77-80.

Interface Structure, Mechanical Properties of Si_3N_4 Nanocomposites

906C7512 Tokyo SERAMIKKUSU KISO KAGAKU TORONKAI in Japanese 24 Jan 90 p 41

[Article by Kansei Izaki, Mitsubishi Gas Chemicals Co., Ltd.; Katsuaki Suganuma, National Defense Academy; and Kooichi Niihara, Sanken (ISIR), Osaka University]

[Text] **1. Objective**

The research and development of a composite with superior mechanical properties of both Si_3N_4 and SiC by means of dispersing particles and whiskers of the latter in the former are being pushed ahead globally. The authors, in turn, have recently succeeded in turning out a nanocomposite material, a composite in which very fine particles of SiC with a diameter from several score to a hundred nanometers are dispersed inside particles of Si_3N_4, by using, as the starting material, an Si-C-N composite precursor powder produced by CVD. The composite displays a strength of some 1,000 MPa even at a temperature of 1,400°C. This report deals with correlations among the method of manufacture of Si_3N_4/SiC nanocomposite, its micro- and nanostructures, and its properties such as strength, toughness, and high-temperature strength, and with a discussion on the role played by the SiC particles dispersed in the Si_3N_4 grains and in its grain boundaries on the basis of transmission electron microscope (TEM) pictures observed.

2. Method of Experiment

Hexamethyl-disilazane and ammonia were allowed to react in vapor phase at 1,000°C and then subjected to a thermal treatment for 4 hours at 1,350°C under N_2 flow, such that several kinds of SiC-C-N composite powders having different C/N ratios and allowing handling in air were yielded. The composite powder, together with the sintering promoter Y_2O_3/Al_2O_3 or Y_2O_3, were subsequently subjected to wet-process mixing with Si_3N_4 balls and to hot pressing under N_2 at a pressure of 34 MPa and a temperature of 1,700~1,800°C to give a sintered compact. The phases constituting the sintered compact were identified by X-ray diffraction and the micro- and nanostructures were observed with scanning electron microscope (SEM), TEM, an electron microscope of high resolution, etc.

3. Results and Discussion

Observation with the electron microscope showed that SiC particles with a diameter below 0.1 μm were located in the crystal grain of the Si_3N_4, and those with sizes above that level were in the grain boundary. It was also shown that, at the interface between Si_3N_4 and the SiC located in the Si_3N_4 grain, no definite phases due to a contaminating material were observable independently of the kind of sintering promoters applied, but that, at the interface between Si_3N_4 and the larger-size SiC located within the grain boundary of Si_3N_4, the presence of the phase of contaminating material depended on the kind of sintering promoters used, and the use of Y_2O_3 alone as the promoter allowed direct bonding of the two phases of Si_3N_4 and SiC. The results of SEM observation of fractured surfaces of the composite, in turn, led to the conclusion that the shape of the Si_3N_4 grain in the composite depended heavily on the amount of SiC—the grain growing in rod form when the amount is limited, and growing more isodiametrically in shape and more fine in size as the amount increases.

As for the toughness of the nanocomposite SiC/Si_3N_4, it grew with an increasing amount of SiC up to 25 percent in volume of the material, but declined beyond that level. The fracture strength, in turn, showed changes similar to that of toughness, reaching levels as high as 1,500 MPa or more for an amount of SiC of 25 percent in volume. With strength at high temperature depending heavily on added sintering promoters, composites involving a promoter of Al_2O_3/Y_2O_3 series exhibited a pronounced decrease in strength at temperatures above 1,300°C, whereas those containing Y_2O_3 alone as the promoter displayed a high strength of above 1,000 MPa at 1,400°C and some 900 MPa even at 1,500°C. A discussion of the high-temperature strength and the grain boundary structure will be given in further detail in the coming lecture.

High-Temperature Properties of MgO-Based Nanocomposites

906C7512 Tokyo SERAMIKKUSU KISO KAGAKU TORONKAI in Japanese 24 Jan 90 p 42

[Article by Koichi Niihara, Sanken (ISIR), Osaka University; Atsushi Nakahira, National Defense Agency; Hiseo Ueda, Hiroshi Sasaki, and Ryuu-ichi Matsuki, Mitsubishi Kogyo Cement (Mitsubishi Mining and Cement Manufacturing) Co., Ltd.]

[Text] **1. Introduction**

Although MgO is an excellent ceramic in terms of heat resistance and thermal conductivity, its mechanical properties such as strength and toughness are not satisfactory and need to be improved if it is to be used in practical applications. Previous reports have demonstrated that dispersion of very fine particles of SiC in the grains of MgO, to give the so-called nanocomposite, is very effective in improving the properties of MgO and allows a pronounced advance in its mechanical properties. This report deals with mechanical properties such as strength, toughness, and hardness at high temperature of the nanocomposite MgO/SiC.

2. Experiment

The materials used were a high purity MgO made by Ube-Kosan Co., Ltd., and an SiC, 5~50 percent in volume, made by Ibiden Co., Ltd., which were mixed in ethanol with the ball mill. The mixed powder was then subjected to hot pressing at 1,700~1,900°C under argon atmosphere. The resultant sintered compact was cut in size to 3 x 4 x 36 mm, ground, and lapped to give specimens for measurements. The density was estimated by the Archimedes' method, Young's modulus by the resonance method, and fracture toughness by the IM method and the Shebron notch method. The fracture strength measurements were carried out by three-point bending test in air at temperatures up to 1,400°C, and the hardness measured in the Vickers hardness unit in the range of room temperature to 1,300°C by use of a high-temperature microscopic hardness-meter (made by Nikon, QM type). The microstructure of the composite was observed by transmission electron microscope (TEM) and scanning electron microscope (SEM).

3. Results

Observations by TEM and SEM showed that the SiC particles with a diameter 0.2 μm or less occurred in the matrix MgO grains, and those with a larger diameter did in its grain boundaries. An observation with an electron microscope of high resolution also confirmed the absence of any contaminant phases at the interfaces between MgO and SiC phases.

The composite with SiC added in, 50 percent in volume, exhibited a strength of 750 MPa, a value twice or more that for the simple ceramic MgO, and had a toughness about four times larger than the latter. The hardness increased when an increasing amount of the SiC was involved. The pronounced feature in the nanocomposite MgO/SiC was that the strength at room temperature was sustained up to high temperatures of 1,300~1,400°C and that strength at high temperatures are enormously improved. Figure 1 presents plots of the hardness of the composite at high temperatures. The mechanism of improvement of the mechanical properties will be reported in detail at the coming meeting.

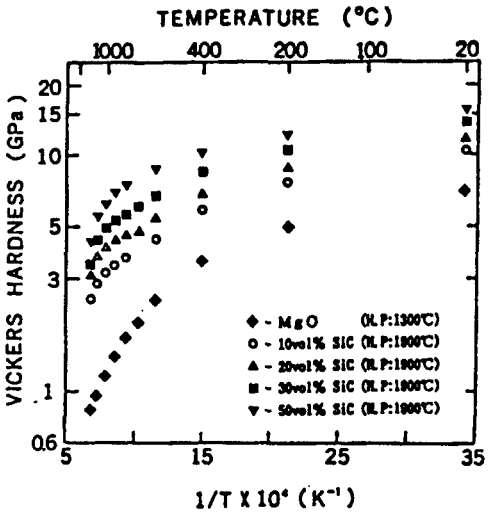

Figure 1. Hot Hardness of MgO/SiC Nanocomposites

HIP Sintering of Si_3N_4-SiO_2 Ceramics

906C7512 Tokyo SERAMIKKUSU KISO KAGAKU TORONKAI in Japanese 24 Jan 90 p 67

[Article by Jianren Zeng, Isao Tanaka, and Toshinari Miyamoto, Sanken (ISIR), Osaka University, and Osamu Yamada, Osaka Industrial University]

[Text] **1. Introduction**

A previous article of the authors reported that Si_3N_4 with added high-purity SiO_2 had its strength sustained up to a temperature of 1,400°C. The addition of SiO_2 to Si_3N_4 provides the best means for exploring the behavior of HIP sintering for Si_3N_4 and the basic properties of the resulting compact, since the quantity of Si_3N_4 glass in the grain boundary is controlled without changing its quality by the addition of SiO_2. The present article deals with an investigation into the compacting process and phase transformation behavior of Si_3N_4 in the HIP sintering and effects of addition of SiO_2 on the high-temperature properties of the resulting composite, and with a discussion of these properties of the composite in relation to its microstructure.

2. Specimens

High purity SiO_2 (made by Hokkou Kagaku Co., Ltd.) was added in 2.5, 5, 20, 30, and 80 percent by weight to high purity Si_3N_4 powder (containing 2.5 weight percent SiO_2, made by Ube Kosan Co., Ltd.) and subjected to wet mixing, drying, and CIP molding at 200 MPa, followed by vacuum sealing into a Pyrex glass and then by HIP sintering at 1,700~2,000°C without adding any sintering promoters.

3. Results and Discussion

As can be seen from Figure 1, with an increasing amount of addition of SiO_2, the compacting process was increasingly enhanced and, conversely, the transformation of phase from α to β was increasingly delayed. With specimens with SiO_2 added in 20 percent by weight, for example, the compacting process nearly completed without appreciable phase transformation at a temperature of 1,800°C. Near absence of grain growth in the resulting composite suggests that the compacting process was achieved by grain rearrangement only. The delaying of the phase transformation by the presence of SiO_2 in the composite may be understood thoroughly by assuming that diffusion in the SiO_2 glass works as the

rate determining process in the dissolution and deposition process of the α phase. Figure 2 presents the effects of addition of SiO_2 on the strength of the composite as measured by the JIS four-point bending test at 1,400°C. Addition of SiO_2 in 10 percent by weight did not allow the high-temperature strength of the composite to fall, indicating that the relevant fall seen in common Si_3N_4 results from contaminants other than O_2. Specimens with SiO_2 added in 20 percent by weight or over, however, showed plastic deformation: a major difference in deformation behavior was observed between the specimens with SiO_2 added in 10 percent by weight and those with the relevant addition above that level, even if the strain rate was decreased to one-tenth and one one-hundredth, which suggested that the microstructure of the Si_3N_4 changed from a cross-linkage state to a mutually isolated state.

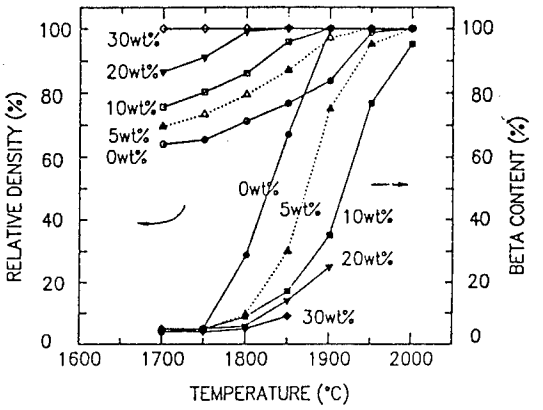

Figure 1. Relative Densities and β-Phase Contents of Si_3N_4-SiO_2 HIP Sintered at 170 MPa for 1 Hour

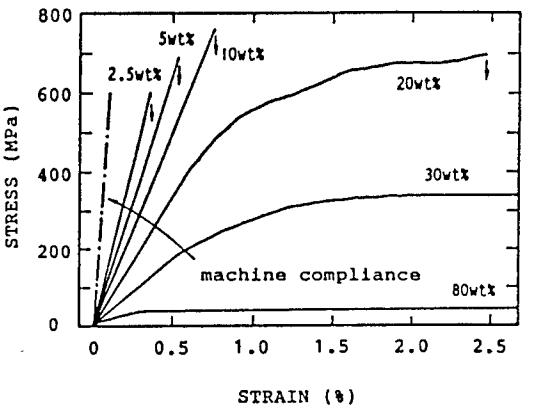

Figure 2. Stress-Strain Curves of Four-Point Bending Test at 1,400°C at Outer Fiber Strain Rate of 1.5 x 10^{-4}/s

Reaction Analysis of Combustion Synthesis--(1) TiC, TiB_2

906C7512 Tokyo SERAMIKKUSU KISO KAGAKU TORONKAI in Japanese 24 Jan 90 p 72

[Article by Osamu Yamada, Liberal Arts College, Osaka Industrial University, and Toshikazu Takakura and Yoshinari Miyamoto, Sanken (ISIR), Osaka University]

[Text] **1. Introduction**

As reported in previous articles by the authors, combustion synthesis allows preparation of various high-melting ceramics and intermetallic compounds and, besides, simultaneous synthesis and sintering of ceramics by application of external pressures during the reaction. It is, nevertheless, far from easy to control relevant combustion reaction, which is necessary for adjusting the speed and temperature of combustion and lowering the external pressure to be applied. With the view to attaining this objective, the authors first estimated the activation energies of representative nonoxide ceramics and studied the basic reaction-rate determining process for the combustion synthesis.

2. Method of Evaluating Activation Energy E

Although actual combustion reaction is substantially complex, an analysis of the reaction is possible in simple reaction systems by measurement of combustion-plane propagation speed, etc. Assuming that, in a combustion reaction of a condensed system in the steady state, the chemical reaction takes place in the very narrow region of high temperature at $T = T_{max}$ in the vicinity of the plane of combustion, then the propagation speed of the combustion plane may be represented by the formula

$$ln\left(\frac{U\rho}{T_{max}}\right) = \left(\frac{-E}{2R}\right) * \left(\frac{1}{T_{max}}\right) + Const.$$

where $U\rho$ denotes the propagation speed of the combustion plane (mole/$cm^2 \cdot$sec) and T_{max} the maximal temperature reached during the combustion. The activation energy E of the combustion was then estimated by plotting in the Arrhenius type of $ln\left(\frac{U\rho}{T_{max}}\right)$ *vs.* $\frac{1}{T_{max}}$. The T_{max} was varied by changing the amount of the product mixed in the raw material preliminary as the diluent.

3. Results

Activation energy E for each of the systems is shown in Table 1. The table also gives the adiabatic combustion temperature T_{ad}, the melting point of the reactant (denoted by m, relevant element given in parentheses), and the melting point of the product (denoted by M, relevant compound given in parentheses). Where TiB_2 is concerned, its phase alone remains as solid in combustion, since the temperatures for the species involved for the experimental range were of the order m(Ti), $m(B) < T_{ad} < M(TiB_2)$. The energy E proved to be 285 kJ/mol. As previously reported, the reaction mechanism was assumed to involve development and growth of TiB_2 nuclei from the mixture solution of Ti and B; a calculation of the activation energy for the nucleus development proved the value to be very small and hence the process to not determine the reaction-rate. In the case of TiC, the two phases C and TiC are in the solid state during combustion in the experimental range. The activation energy was a high 842 kJ/mol, which was too high a value to be accounted for by the rate determining process caused by material transfer alone and hence the question of thermal transfer is now being studied.

Table 1. Activation Energy E Calculated From the Combustion Speed

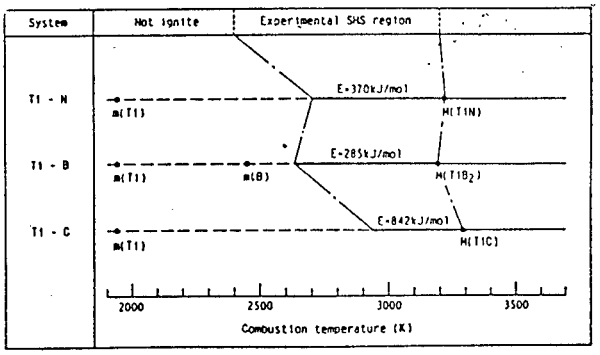

Sintering of Ceramics by Self-Combustion Synthesis

906C7512 Tokyo SERAMIKKUSU KISO KAGAKU TORONKAI in Japanese 24 Jan 90 p 73

[Article by Takashi Shiono, Nobuyuki Komura, Toshihiko Nishida, and Tomozou Nishikawa, Faculty of Engineering and Design, Kyoto Institute of Technology]

[Text] **1. Introduction**

Nitrides, carbides, borides, etc., in general, involve formation heat of ten to several hundred joules per mole, and hence, liberate large quantities of heat in the course of their formation. Research is therefore currently underway to allow this formation heat to work in the sintering of these compounds, which are hardly amenable to the processing, such that the sintering be completed with use of lesser amounts of heat and without the use of any sintering promoters. The present research is aimed at preparation of Al_2O_3–AlN composites at low temperature by use of Al_2O_3 and Al powder as the starting materials and by use of the reaction heat generated during nitridation of the aluminum and at investigation of the ratio of mixing of the raw materials, the sintering temperature, the period of sintering, etc.

2. Experiment

Commercially available Al_2O_3 powder with an average diameter of 0.22 μm and Al powder with an average diameter below 44 μm were used as the starting materials. To the Al_2O_3 was added the metal aluminum powder in 30~70 percent by weight and then subjected to dry ball-milling for 24 hours. The mixture was molded under pressure into a square columnar form, such that the relative density of the mold was 60 percent and, subsequently, the reaction was allowed to take place under an N_2 stream of 200 mℓ/minute, at a rate of temperature rise of 5°C/minute, at a sintering temperature ranging from 660~900°C, and for a sintering period from 0~10 hours. For individual specimens with a different ratio of raw-material mixing, the rate of conversion from Al to AlN was measured for varying temperatures and times; identification of the phases involved by X-ray diffraction and observation of the microstructure with the scanning electron microscope (SEM) was carried out.

3. Results

The figures present plots of the rate of conversion from Al to AlN vs. the sintering time for different sintering temperatures and for the amount of addition of Al of 40~50 percent by weight. Where the amount of Al added was 50 percent by weight, the rate of nitridation increased with increasing sintering temperature and increasing sintering time, reaching 100 percent in 10 hours when sintered at 660°C and in 3 hours when sintered at 800~900°C. Where the metal Al was added in 40 percent by weight, compacts with a rate of nitridation of 100 percent were afforded in 5 hours when sintered at 660°C, but, in contrast to the above, the rate fell with the higher sintering temperature cases: moreover, where the amount of Al added was 30 percent by weight or less, no nitridation took place. It was inferred that the fall of the nitridation rate with decreasing amount of Al might result from the reaction heat generated in the formation of AlN being lost to the surrounding Al_2O_3, and thus a chain reaction of AlN synthesis being blocked.

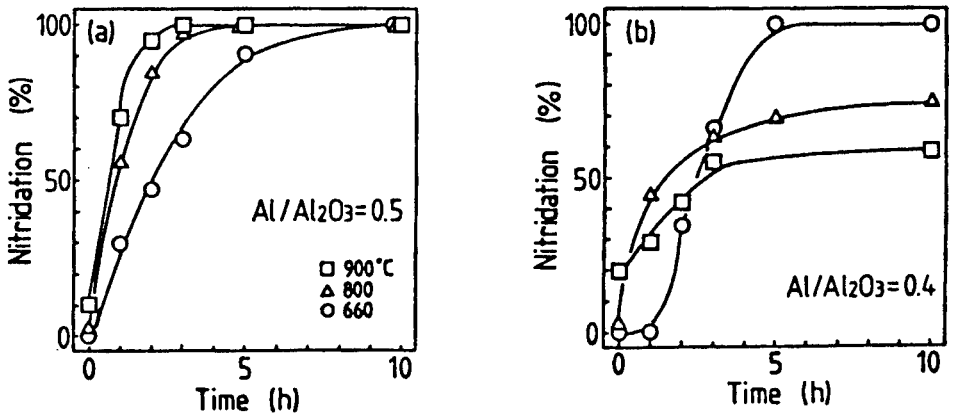

Figure 1. Plot of Rate of Nitridation Vs. Time for Nitridation for Different Sintering Temperatures (and for different Al to Al_2O_3 ratios)

X-ray diffraction analysis of the compacts with low nitridation rates showed that every specimen with different raw material combination ratios has the nitridation ratio rising as the site of the test when deeper in the compact, which may conceivably result from the heat generated in the internal part being more difficult to be liberated than the one produced at the surface. No phases other than those of Al, Al_2O_3, and AlN was observed in the specimens having completed the reaction.

Properties, Preparation of Porous Body of SiC

906C7512 Tokyo SERAMIKKUSU KISO KAGAKU TORONKAI in Japanese 24 Jan 90 p 74

[Article by Yushi Yamamoto, Yoshiyuki Miyaji, and Hajime Izawa, Advanced Material Research Laboratory, Osaka Cement Co., Ltd.]

[Text] **1. Introduction**

Inorganic porous bodies have a good prospect of application in advanced technologies because of their superior resistance to heat, corrosion, radiation, etc. In the present research, a carbon-silicon carbide (C-SiC) compact prepared by combustion sintering was subjected to the removal of its carbon component to give a silicon carbide porous body, of which a report on the method of manufacture and the properties are to follow.

2. Method of Experiment

Carbon and silicon materials molded in given forms were allowed to react under argon atmosphere at 1,800°C to give a composite comprising carbon and silicon carbide, which was then subjected to heating under air at 1,000°C for 3 days, such that the carbon part could be removed by oxidation and that a porous silicon carbide body could be given. Observation of the microstructure of the porous body was conducted by scanning electron microscope (SEM), and identification of the crystal phases involved by means of X-ray diffraction.

3. Results

In the X-ray diffraction picture of the composite, diffraction lines of β-silicon carbide and silicon were noted, the latter weakly, in addition to that of carbon, whereas, in the picture for the porous body, the carbon line was gone with weak lines of β-silicon carbide and silicon remaining. Figure 1 presents an SEM photo of the fractured surface of the compos-ite, an EPMA photo of the distribution of silicon in the same visual field, and an SEM photo of the porous body fractured surface. Comparison of the first SEM photo with the second for Si distribution in the same visual field showed that silicon carbide was distributed there as if it surrounded carbon parti-cles of sizes 10~100 μm that made up the carbon material. The third photo, in turn,

proved vacant spaces of sizes 10~100 μm continuing, which resulted from the disappearance of the carbon particles.

(a) (b) (c)

Figure 1. (a) SEM Photo of Fractured Surface of Composition
(b) EPMA Photo of Silicon Distribution in Same Visual Field
(c) SEM Photo of Porous Body Fractured Surface

Preparation, Morphology of Coil-Like Carbon Fiber Grown by CVD

906C7512 Tokyo SERAMIKKUSU KISO KAGAKU TORONKAI in Japanese 24 Jan 90 p 113

[Article by Masayuki Kawaguchi and Koji Nozaki, Central Glass Co., Ltd.; Seiji Motoshima, Gifu University; and Hiroshi Iwanaga, Liberal Arts College, Nagasaki University]

[Text] **1. Introduction**

Carbon whiskers useful as a material for composites are generally prepared from the raw material benzene by means of chemical vapor deposition (CVD) at a high temperature of 1,000~1,300°C with use of a transition metal, for example, iron or nickel, as the catalyst. As yet, there is little detailed research on the synthesis of whiskers at temperatures below 1,000°C. In the present investigation, the authors produced a carbon fiber at temperatures below 1,000°C from the material acetylene, C_2H_2, which is readily decomposed thermally at lower temperature, and investigated the effects on properties and shapes of the fiber when conditions for the synthesis were varied.

2. Experiment

A substrate or powder of nickel was set at the center of a horizontal flow-through type tube-like furnace (made of quartz) and, after having made the tube oven vacuous and electrically raised the temperature within to a given level, C_2H_2 diluted with either H_2 or argon was introduced to allow the gas to react for 1 hour. The resultant product was examined by X-ray diffraction, scanning electron microscope (SEM), transmission electron microscope (TEM), etc.

3. Results and Discussion

It was shown from examination that carbon fibers were yielded at temperatures from 350~900°C and that parts of the fibers were wound regularly in coil form, as seen in the photograph of Figure 1. The coil was often wound doubly in the same direction with a nickel compound located at the terminal of the coil, which may conceivably work as the catalyst.

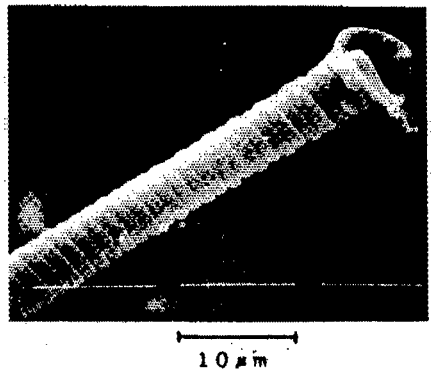

Figure 1. SEM Photo of Carbon Fiber in Coil Form

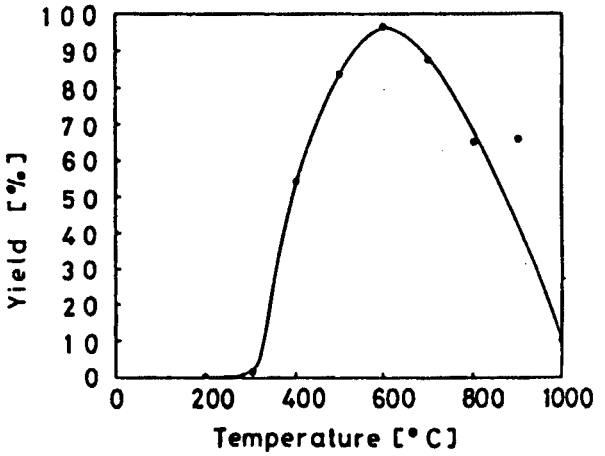

Figure 2. Plot of Yield in Percent Vs. Temperature in Degrees Centigrade for Carbon Fiber (linear and coil forms)

Figure 2 presents a plot of the temperature for the synthesis of the fiber vs. the yield of both the linear and the coil forms. The maximal (total) yield was reached at 600~700°C, as was the yield of the coil-form fiber (maximum yield of coils is now 20 percent).

It was also shown that coil-form fibers yielded at 700°C sustained their shape after a thermal treatment even at 2,000°C.

Morphology, Spring Characteristics of Si_3N_4, Carbon Fiber

906C7512 Tokyo SERAMIKKUSU KISO KAGAKU TORONKAI in Japanese 24 Jan 90 p 114

[Article by Hiroshi Iwanaga, Liberal Arts College, Nagasaki University; Seiji Motojima, Engineering Department, Gifu University; and Masayuki Kawaguchi, Central Glass Co., Ltd.]

[Text] **1. Silicon Nitride in Coil Form**

Silicon nitride fibers were produced from a raw material mixture of the gases Si_2Cl_6, NH_3, H_2, and Ar with some very small amounts of contaminant metal added by means of a contaminant-activation CVD at a temperature of 1,200°C. Where the contaminant graphite/Fe was applied, a silicon nitride wound regularly in coil-form was yielded as shown in Figure 1. The coil had a constant coil pitch of 2~5 μm and a constant coil diameter of 20~30 μm, and exhibited knotty deposits thereon at intervals in the coil line. Electron beam diffraction photographs showed the fiber to be made up of an amorphous material by showing a halo pattern.

Figure 1.

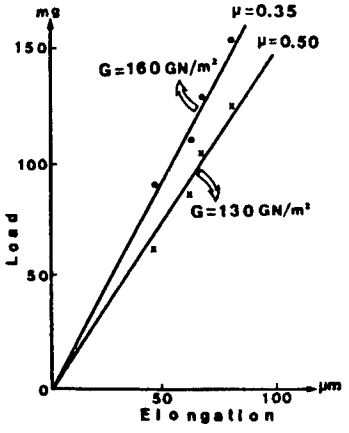

Figure 2.

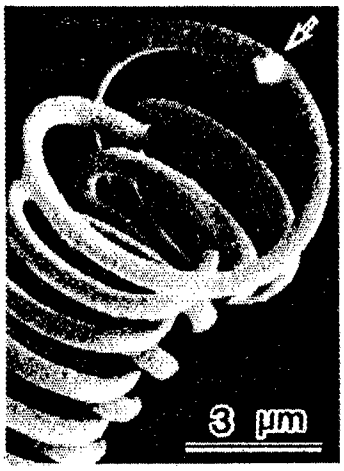

Figure 3.

Figure 2 presents a plot of the elongation of the coil vs. the applied load. By applying the formula $W = 235 (\sin \theta - \mu \cos \theta)$ (mg), and by measuring load W and elongation δ, and thus the incline of the plotted line, the modulus of

elasticity of the fiber was shown to be 130~160 GP. The maximum stress for rupture of the spring was also shown to be approximately 3.0 GP, assuming $r = 12\ \mu m$, $d = 2.8\ \mu m$, and $n = 5$ for the coil.

2. Carbon Coil

Carbon fiber in coil form was formed by thermal decomposition, in the temperature range of 350~700°C, of a mixture of the gases C_2H_2, H_2, and Ar blown over an Ni substrate. The fiber was made up of two coils with the terminal in the shape of the figure 8. A reflection electron picture with the scanning electron microscope (SEM) showed a glowing object at the terminal, as shown in Figure 3, which was identified as an Ni compound from measurements using EPMA. It is conceivable, therefore, that the Ni of the Ni compound worked as a contaminant activator and allowed carbon atoms to be brought out and piled up on both sides of the Ni in coil form. The carbon coil, after having been elongated some 4.5 times its original length, ruptured, and the ruptured piece remained in the elongated state, indicating that a plastic deformation took place; it returned to its original length, however, after it had been stretched three times, which showed that elastic deformation alone is involved in this extent of elongation.

Dielectric Properties of BN-C Thick Films

906C7512 Tokyo SERAMIKKUSU KISO KAGAKU TORONKAI in Japanese 24 Jan 90 p 116

[Article by Shigenobu Yokoshima, Takashi Goto, and Toshio Hirai, Institute for Metal Material Research, Tohoku University]

[Text] **1. Introduction**

Boron nitride, BN, a material finding widespread application in electrical insulation at high temperatures, is largely used in nonoxidizing environments, for example, in the presence of carbon. A clarification of the electrical properties of BN–C is therefore important. It is also yet to be known whether the carbon in BN–C materials exists as a solid solution in BN or as the second phase. In the present research, BN–C thick films were synthesized by CVD, their dielectric properties measured, and the state of the carbon present in the BN–C was studied, of which a report follows.

2. Experiment

A BN having 0.2~2.4 percent by weight of carbon was synthesized on a graphite substrate by CVD from the material gases BCl_3, NH_3, CH_4, and H_2; measurements were taken for the dielectric properties and direct-current conductivity of the resulting BN–C material in the temperature range of 0~800°C with an LCR meter and with a pico ammeter.

3. Results

Figure 1 presents a plot of the dielectric loss for a BN–C specimen involving 0.1 percent by weight of C vs. the relevant frequency. The relationship between log ϵ'' and log f was linear, suggesting hopping conduction. Figure 2 presents plots of the tan δ vs. the frequency for a BN–C with 2.4 percent by weight of C; at any temperature, the loss tangent exhibited the maximum value at some frequency. The maximum frequency f_{max}, increased with increasing temperature, and the relationship between log f and 1/T was linear. The value of activation energy was about 0.2 eV, approximately corresponding to that of C in a staggered layer structure. It was inferred from measurement of dielectric properties of the BN–C materials produced that carbon in the material was

present in a solid solution state, where the carbon content was 0.7 percent by weight or less, and dispersed as the second phase, where the content was 1.0 percent by weight or more.

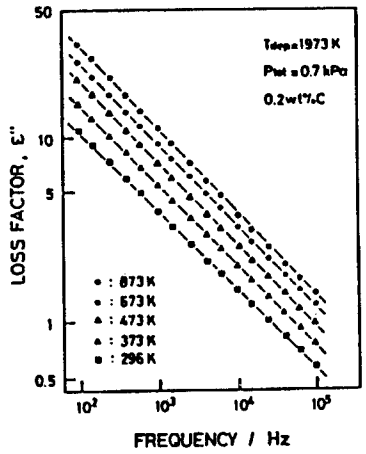

Figure 1. Plot of the Loss Factor ϵ" Vs. Frequency

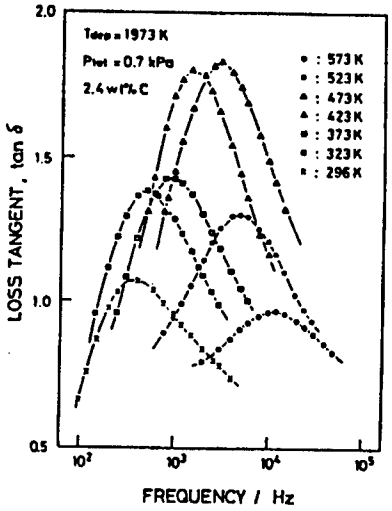

Figure 2. Plot of Tan δ Vs. Frequency

Microstructures of Transition Metal Nitride Films Prepared by CVD

906C7512 Tokyo SERAMIKKUSU KISO KAGAKU TORONKAI in Japanese 24 Jan 90 p 117

[Article by Hiroshi Funakubo, Nobuo Kieda, Motonori Kato, and Ikyo Mizutani, Faculty of Engineering, Tokyo Institute of Technology]

[Text] **1. Introduction**

Several reports have been made on the superior properties exhibited by thin films of composites made up of two nitrides. In preparing, by CVD, iron nitride thin film, which is a prospective material for magnetic recording,[1] the authors allowed titanium nitride to deposit simultaneously, with the view to improving mechanical and chemical properties of the film.[2] Because it is essential for understanding the properties of the film to elucidate its microstructures, the authors observed the microstructure of the film of the composite titanium nitride–iron nitride in its early stages of deposition with an analytical electron microscope, and studied the relationship of its microstructure to that of the fully grown film.

2. Method of Experiment

The thin film was prepared from the materials $Fe(C_5H_5)_2$, $TiCl_4$, NH_3, and H_2 by the heated CVD method with a normal pressure hot-wall-type apparatus. With the temperature of the deposition reaction set at 750°C, the total flow rate at 4.0 ℓ/minute, the pressure of NH_3 at 0.025 atmosphere, and that of H_2 at 0.22 atmosphere, and with the pressures of $Fe(C_5H_5)_2$ and $TiCl_4$ being varied, thin films with different ratios of Ti to Fe were produced. The specimens for transmission electron microscope (TEM) were produced by separation from the substrate of thin films prepared in a short time.

3. Results and Discussion

Figure 1 presents a TEM picture of the above composite with the ratio of Ti and Fe of about 28:72 and a result of its EDS analysis. With synthesis carried out for 45 seconds, the thin film exhibited deposits of around 500~2,000 Å scattered therein. The composition of the deposit (A), was high in Fe, whereas that of the matrix (B), was high in Ti.

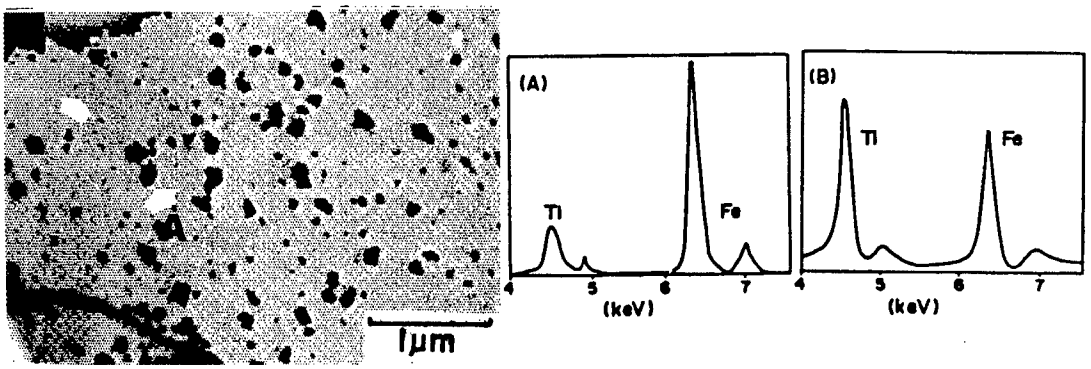

Figure 1. TEM Picture of a Titanium Nitride-Iron Nitride Composite Film and Relevant EDS Analysis Patterns

Such deposits were also observed in the films with the ratio of Ti to Fe different from that of the one in Figure 1, but not in the ones consisting of titanium nitride or iron nitride alone. It is, therefore, conceivable that the microstructure of the figure is unique to the composite thin film. The presence of regions where the composition showed different ratio of Ti to Fe was also noted in thin film specimens of about 1 μm in thickness prepared under the same conditions as those for the one in the figure. Changes of the relevant composition in the direction of the thickness of the film are now under investigation by observation of fractured surfaces of the film.

References

1. Funakubo, H., et al., J. MATER. SCI. LETT., Vol 7, 1988, pp 851-852.

2. Ibid., 1989 Preliminary Manuscripts for the 1989 Annual Meeting of the Japan Ceramics Institute, 1989, p 497.

Effects of Substrates, Holders on Preparation of Diamond by Plasma CVD

906C7512 Tokyo SERAMIKKUSU KISO KAGAKU TORONKAI in Japanese 24 Jan 90 p 118

[Article by Hisako Hirai, Youichi Yazaki, and Osamu Fukunaga, Department of Inorganic Materials, Tokyo Institute of Technology]

[Text] **1. Introduction**

Although it is well known that properties of diamond prepared by the vapor deposition method are dependent on properties and surface conditions of the substrate used, few cases of research are available on the effect of the holder on which to set the substrate. In the microwave plasma method, both the substrate and the holder are subjected to dielectric and induction heating and to heating from impact by the bombardment of plasma. Conduction of heat from the holder to the substrate cannot be ignored in connection with the substrate temperature. It is also conceivable that the holder, when subjected to thermal decomposition, affects reactive species in the plasma. The present investigation is aimed at eludicating the effects of different holder materials on the heat conduction from the holder to the substrate and on the kinds of chemical species supplied.

2. Experiment

Single crystals of Si were used as the substrate (8 x 8 x 0.5 mm). The holder materials were natural pyrophyllite, quartz glass, a sintered compact of alumina, graphite, hBN, and Mo, which were machined into a cylinder 16 mm in diameter and 16 mm in length. With application of pressures of 30, 40, and 50 torr, the output of the 2.45 GHz frequency microwave was varied from 100~1,000 W so that the relationship between the output and the temperature of the substrate could be studied; temperature was measured with an infrared-ray emission thermometer. The diamond synthesis was carried out from the material CH_4/H_2 (CH_4 concentration of 0.06 percent, gas pressure of 30 torr) at a substrate temperature of 850°C.

3. Results and Discussion

Even if the microwave output stays constant, the values of the substrate temperatures vary widely, depending on the material of the holder, in the

range of, for example, 100°C for the output of 800 W. The substrate temperature is influenced not only by the specific permittivity and dielectric loss, but also by heat conductance to the holder, the temperature falling with rising heat conduction of the holder. With other conditions being identical, the diamond thus formed varies widely, depending on materials of the holder, in terms of nuclei-development rate, size, shape, crystallinity, and contaminants, as exemplified by Figures 1 and 2. The concentrations of carbon and contaminants in the plasma may conceivably be affected by the substrate holder. In the case of graphite holders, (100) face of the crystal is dominant, in agreement with the high CH_4 condition, whereas, in pyrophyllite holders, fluorescence in the Raman spectrum is extraordinarily high and the diamond peak is weak, suggesting the presence of contaminants. From this, it was concluded that the holder may be available as an auxiliary heater and cooler by selecting proper materials for it and designing a proper method of holding, and that it may also be available as a source of doping elements.

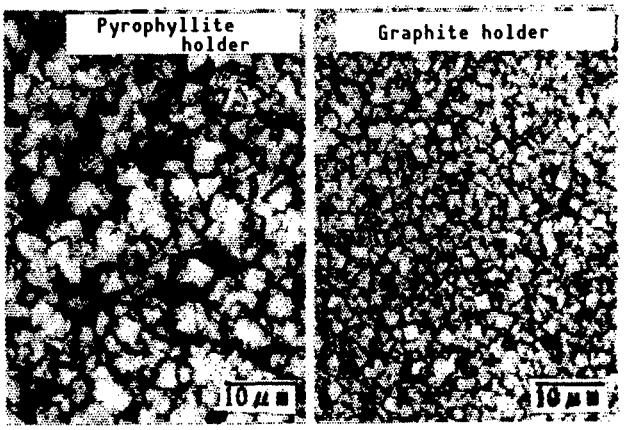

Figure 1. Reflection of Microscopic Picture

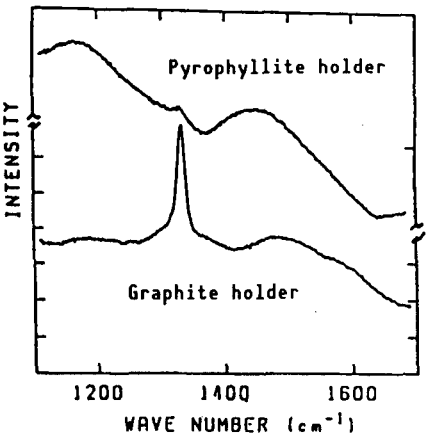

Figure 2. Raman Spectrum

Preparation of Rf-Sputtered Amorphous Aluminum Oxynitride Films

906C7512 Tokyo SERAMIKKUSU KISO KAGAKU TORONKAI in Japanese 24 Jan 90 p 124

[Article by Toichi Hanada, College of Liberal Arts and Science, Kyoto University, and Masahiro Kobayashi and Naohiro Soga, Faculty of Engineering, Kyoto University]

[Text] **1. Introduction**

Aluminum nitride with its superior piezoelectric properties and a wide bandgap is a prospective material for surface-acoustic-wave devices operating in the high frequency range and for optical devices operating in the ultraviolet region, as well as for electrical insulation and for passivation of semiconductors. It seems that preparation of the material is affected by contamination of the relevant atmosphere with slight amounts of oxygen. In this research, therefore, an amorphous film of the material was trial manufactured by Rf sputtering, using aluminum nitride powder or aluminum plates as the sputtering target and nitrogen gas as the sputtering gas. With the resultant film involving contaminant oxygen in large amounts, as suspected, the contents of nitrogen and oxygen in the film were measured such that the relationship between the O/N ratio and the sputtering conditions were revealed; the density of the film was also measured.

2. Method of Experiment

A radio frequency sputtering apparatus (made by Nippon Shinku, SBR-1104) was used for preparing the specimens. Sputtering was carried out under the condition given in Table 1 with use of an AlN powder made by Toyo Aluminum Co., Ltd., for the target and a high purity nitrogen gas for the sputtering gas. X-ray diffraction was used for determining the amorphous state, and a Horiba oxygen-nitrogen analyzer, EMGA-650, for measurement of the contents of the nitrogen and oxygen in the film.

3. Results

Table 2 presents the O/N ratios of films produced under different sputtering conditions. As can be seen, the oxygen content was lower with lower gas pressures and with use of the aluminum target. The content also dropped with

use of a liquid nitrogen trap in the diffusion pump. These results showed that the oxygen content was heavily dependent on sputtering conditions. the density of the oxinitride produced was found smaller than that for amorphous aluminum oxide.

Table 1. Sputtering Conditions

Target	AlN, Al
Sputtering gas	N_2
Gas pressure	3 Pa, 0.8 Pa
Rf power	100 W
Substrate	Cu plate, slide glass
Substrate temperature	20~40°C

Table 2. O/N Ratio in Films

Number	Target	Pressure (Pa)	Liquid N_2	O/N ratio
1	AlN	3	No	1.62
2	AlN	0.8	No	0.89
3	AlN	3	Yes	0.71
4	Al	3	No	0.81
5	Al	0.8	No	0.66

No-Hysteresis Piezoelectric Actuator

906C7512 Tokyo SERAMIKKUSU KISO KAGAKU TORONKAI in Japanese 24 Jan 90 p 160

[Article by Hiroshi Asakura and Hiroshi Yamamura, TOSO Corp.]

[Text] **1. Introduction**

In cases where displacements are controlled by electric potential with use of a piezoelectric actuator, a hysteresis phenomenon generally takes place in the amount of displacement between the rising and falling courses of the potential applied. Because of this hysteresis, a change in the value of the potential does not produce a single value for the corresponding change in displacement, and some special design such as the polarization value control method or feedback control is necessary. Although their hysteresis wideness is limited, electrostriction materials also do not meet requirements satisfactorily because the relationship between the electric potential and the displacement is not linear and the hysteresis is not gone completely. In the present investigation, the authors invented a design in which a bimorph-type actuator was cleaved for length (that is, transversely) such that the displacement of the terminal part of the bimorph was made free from the effect of hysteresis; thus, its relationship to the potential applied was linear. The device also proved to be capable of providing stable displacement more independently of temperature changes, a report of which follows.

2. Method of Experiment

The piezoelectric plate was produced as follows: Molding into sheets of the raw material powder of a PZT; dewaxing; sintering at 1,230~1,270°C for 2 hours; printing and baking of a silver paste as the electrodes; and, finally, polarization treatment of the resultant product. Four plates of the piezoelectric material produced and a shim plate of phosphorous bronze were pasted with an epoxy binder to give an actuator device (Figure 1). Measurements of the displacement were taken with a noncontacting eddy-current sensor.

3. Results and Discussion

Figure 2 presents a plot of the unipolar-driven potential with a period of 15 seconds vs. the displacement, a linear relationship free of the hysteresis

effect. The bimorph cleaved into two and then being bent in directions opposite to one another, such that the terminal portions share greater hysteresis, and that the hysteresis is counterbalanced will lead to this result. This result is also available in principle for eliminating relevant temperature characteristics. Figure 3 presents the temperature dependence of the maximum displacement for the application of a potential of 40 V. Whereas the variation in the value of the maximum displacement with temperature ranges from −20 to +40 percent of the value at room temperature for a conventional bimorph, the one for the bimorph produced as above was within the range of −2 to +8 percent. The theoretical and optimal designing of the above kinds of devices that are influenced least by hysteresis and temperature requires high levels of processing precision and uniformity because it involves a subtle adjustment for the balance of the positive and the negative.

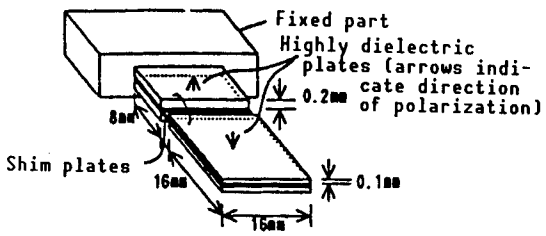

Figure 1. Design of Actuator of Bimorph Type

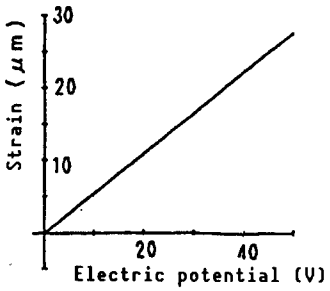

Figure 2. Electric Potential Vs. Strain Curve for Bimorph

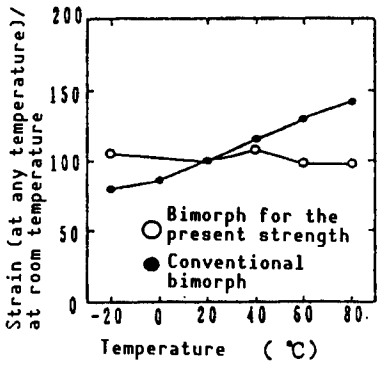

Figure 3. Dependence on Temperature of Strain

Microstructure, Dielectric Properties of Tungsten Bronze-Type Ceramics

906C7512 Tokyo SERAMIKKUSU KISO KAGAKU TORONKAI in Japanese 24 Jan 90 p 161

[Article by Yoji Ueda, Toshio Kimura, and Takashi Yamaguchi, Faculty of Science and Technology, Keio University]

[Text] **1. Summary**

Compacts with different microstructures were produced for an oxide of the tungsten bronze type, $Ba_{0.5}Sr_{0.5}Nb_2O_6$, by varying the particle size and the sintering condition of the powder. This investigation has shown that the way in which their dielectric constants vary with temperature are different from each other and that the differences are related to the microstructures of the composites.

2. Method of Experiment

$BaCO_3$, $SrCO_3$, and Nb_2O_5 were mixed in the ratio 1:1:2 and calcined for 1 hour at 1,200°C. The calcined powder was crushed for 24 hours with zirconia balls 15 mm in diameter, and part of it for an additional 48 hours with ones 2 mm in diameter, thereby preparing two kinds of powder specimens, powders A and B, respectively. The powders were molded into cylindrical form by adding a binder, and then sintered at 1,100~1,350°C for 1 hour. The resultant sintered compacts were provided with In-Ga electrodes, and their capacitance measured in the temperature range from 0~200°C. Their microstructures were determined by scanning electron microscope (SEM) and their lattice parameters by X-ray diffraction.

3. Results and Discussion

Figure 1 presents the temperature dependence of the relative permittivities of these compacts. The Curie point varied in large measure with varying microstructure. In compacts made from powder B, in particular, the dependence of permittivity on temperature was given by a flat curve with the Curie point below 100°C.

Figure 2 represents a plot of Curie point vs. the axial length ratio, c/a. The relationship is linear and it is conceivable from this that the magnitude of the Curie point is related to internal stresses within the particle.

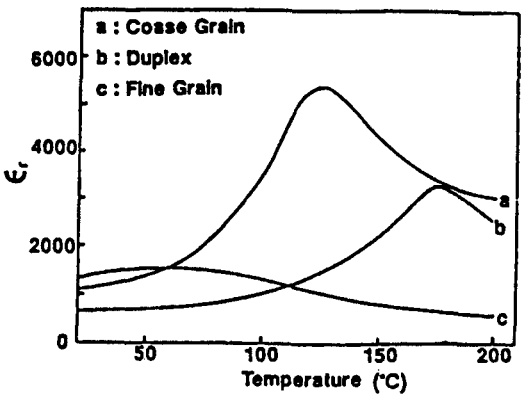

Figure 1. Plot of Relative Permittivity Vs. Temperature

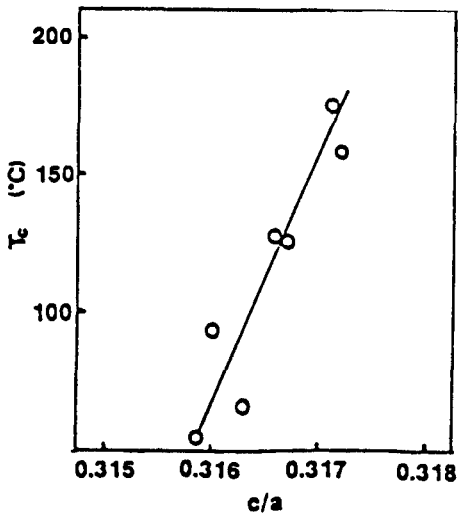

Figure 2. Plot of Critical Temperature (T_c) Vs. Axis Ratio (c/a)

Preparation, Properties of $Y(Ba_{1-x}St_x)_2Cu_4O_8$ Superconductors

906C7512 Tokyo SERAMIKKUSU KISO KAGAKU TORONKAI in Japanese 24 Jan 90 p 167

[Article by Takahiro Wada, Takeshi Sakurai, Nobuo Suzuki, Shinichi Koriyama, Hisao Yamauchi, and Shouji Tanaka, Superconductivity Research Laboratory, ISTEC]

[Text] **1. Introduction**

The superconductor $YBa_2Cu_4O_8$(124 phase) with a critical temperature, T_c, of 80 K is, unlike the $YBa_2Cu_3O_{7-y}$(123 phase), a stable material that involves two CuO chains such that it allows no oxygen to be freed from it upon heating up to 850°C. In the present research, compounds were prepared in which part the Ba of the compound $YBa_2Cu_4O_8$ was substituted by Sr, and the effects of this substitution on the lattice constant and superconductivity of the resultant compounds were examined. The result was also compared with that of the 123 phase, $Y(Ba_{1-x}Sr_x)_2Cu_3O_{7-y}$.

2. Synthesis of the Compounds

Specimens for the compound $Y(Ba_{1-x}Sr_x)_2Cu_4O_8$ were prepared by a solid phase reaction involving high-pressure oxygen treatment. Following sintering under oxygen at 900°C the material was again sintered for 10 hours at 950°C under a gas mixture of argon and oxygen in the ratio of 4:1 at a pressure of 100 MPa by use of an O_2-HIP to give the specimen.

3. Results

For the compound series $Y(Ba_{1-x}Sr_x)_2Cu_4O_8$, the range in which the 124 phase yielded nearly in single phase, was limited in $0 \leq x \leq 0.4$. Figure 1 presents a plot of the Sr content vs. the lattice parameter for the 124 phase and, for comparison, for the 123 phase. In both phases, the lattice parameters a, b, and c fall with increasing Sr content. The 124 phase, in addition, has the feature that the crystal turns more orthorhombic, that is, the ratio b-a/a grows larger, with increasing Sr content.

Figure 2 is a plot of T_c vs. Sr content, as calculated from the resistance-temperature curve, for the 124 phase and, for comparison, for the 123 phase.

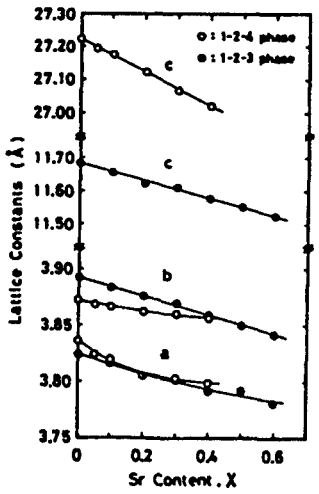

Figure 1. Dependence on Sr Content of the Lattice Parameters

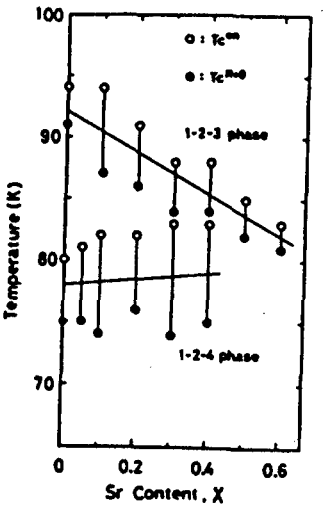

Figure 2. Dependence on Sr Content of the Critical Temperature (T_c)

In the case of the 123 phase, as can be seen, the T_c falls linearly with increasing Sr content, whereas, in the 124 phase, it remains nearly stationary at 80 K independently of the Sr content. An investigation on the decomposition temperature for the 124 phase obtained by thermogravimetrical analysis (TG) will also be reported in the coming meeting.

Preparation, Superconducting Properties of $Y(Ba,La)_2Cu_4O_8$

906C7512 Tokyo SERAMIKKUSU KISO KAGAKU TORONKAI in Japanese 24 Jan 90 p 168

[Article by Takeshi Sakurai, Takahiro Wada, Nobuo Suzuki, Shinichi Koriyama, Takayuki Miyatake, Hisao Yamaguchi, Naomi Koshizuka, and Shoji Tanaka, Superconductivity Research Laboratory, ISTEC]

[Text] The authors were able to control in the range from 40~80 K the critical superconducting temperature, T_c, of $YBa_2Cu_4O_8$ (124) superconductor, which involves two CuO chains, by substituting La for part of Ba. The method of manufacture of the compounds and their properties constitute the present report. It also includes a comparison of these compounds with $(Y,Ca)Ba_2Cu_4O_8$ for superconducting properties.

Takemiya, et al., reported that the superconductor $YBa_2Cu_4O_8$ (124) has its T_c raised by 10~90 K by substituting Ca for part of the Y.[1] On the assumption that the rise of the T_c may have been realized by introduction of holes caused by the Ca substitution, an experiment was carried out to show that substitution of La for Ba, which reduces the number of holes, will allow a drop in T_c. The specimen was produced by a solid phase reaction using high-pressure oxygen atmosphere.

The material powders Y_2O_3, $Ba(NO_3)_2$, La_2O_3, and CuO of above 3N were subjected to dry mixing under inert atmosphere and calcined for more than 10 hours under an oxygen stream at 1,173 K; subsequently, the material was molded into specimens of size 3 x 3 x 20 mm under a pressure of 50 MPa and sintered again for 6 hours under an oxygen stream at 1,223 K. The resulting specimen was shown by powder X-ray diffraction to be a mixture of the $YBa_2Cu_3O_{7-x}$ and CuO phases. This specimen was further allowed to stand under a gas mixture of argon and oxygen in the ratio of 4:1 at a pressure of 100 MPa and a temperature of 1,273 K for 10 hours and then gradually cooled to give the 124 phase.

The presence of a single phase region for the 124 phase was inferred from measurement of the lattice constants by XRD. The c-axis shortened remarkably with increasing amount of La, but stops shortening at $x = 0.1$ in $Y(Ba_{1-x}La_x)_2Cu_4O_8$, which conceivably suggests the limit for the relevant solid-solution formation.

Evaluation of the superconducting properties of the compound was carried out for the single phase region. Figure 1 represents a plot of resistance vs. temperature measured by the direct-current four-terminal method.
For $Y(Ba_{1-x}La_x)_2Cu_4O_8$ with $0 \leq x \leq 0.1$, the specimens, which exhibited metallic resistance changes, have their resistivity increasing and their T_c decreasing in an orderly manner with increasing content of La. At X = 0.0, T_c and $T_c^{R=0}$ were 80 K and 75 K, respectively, but they fell to 60 K and 40 K at X = 0.1. In the range where the amount of La exceeds that for solid solution limit, the T_c became stationary, whereas the $T_c^{R=0}$ declined further. Measurement of direct-current band magnetic ratio also showed that the volume fraction of the superconducting phase fell with increasing content of La.

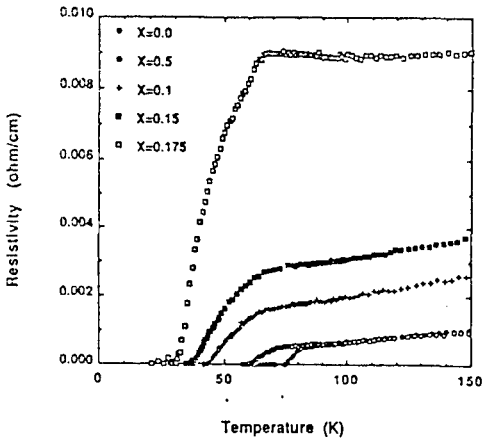

Figure 1. Dependence of Resistivity on Temperature for the Composite $Y(Ba_{1-x}La_x)_2Cu_4O_8$

References

1. Miyatake, T., et al., NATURE, Vol 341, 1989, p 41.

Fabrication, Evaluation of Br-Sr-Ca-Cu-O Superconductors by Sol-Gel Method

906C7512 Tokyo SERAMIKKUSU KISO KAGAKU TORONKAI in Japanese 24 Jan 90 p 173

[Article by Kouichi Yamashita, Masayuki Nagai, Tadashi Nishino, and Takeo Hattori, Musashi Institute of Technology]

[Text] **1. Objective**

The manufacturing methods of oxide superconductors by the solid phase reaction that has so far been employed is confronting limitations in uniformity of the composition of the product and in reduction in size of the particles. The authors, therefore, chose the sol gel method, involving citric acid application, for the manufacture and studied relevant conditions for producing specimens with more uniform composition and more fine-particle size by varying the ratio of the composition and sintering conditions.

2. Method of Experiment

The starting materials Bi_2O_3, $SrCO_3$, $CaCO_3$, and CuO were each weighed so as to give a composition ratio of 2:2:1:2, 2:2:1.5:2.5, and 2:2:2:3. The mixtures of each composition were dissolved in a nitric acid solution as they were heated and stirred, and then citric acid and ethylene glycol, a dispersant, were added with the stirring and heating continued; in the course of this, the solution turned sol after having liberated gases NO_x. The sol was dried, and crushed; it then was calcined at 800°C for 5 hours, crushed again, and its melting point taken by TG-DTA to determine the temperature for subsequent sintering; the resultant materials were molded with application of pressure monoaxially, and subjected to sintering for 20, 40, or 80 hours. Parts of the material thus calcined and crushed were again subjected to calcining and crushing and, having determined the temperature for the subsequent sintering by TG-DTA, were subjected to the sintering for 20, 40, or 80 hours, but for only 10 hours partly. The specimens so produced were subjected to phase identification by X-ray diffraction, to scanning electron microscope (SEM) observation, and to measurement of resistance by direct-current four-terminal method.

3. Results and Discussion

Table 1 presents the results of phase identification by X-ray diffraction. No difference in phase composition was noted resulting from different ratios in composition. After sintering, the superconducting phase proved to be the low temperature phase $Bi_2Sr_2CaCu_2O_x$. A semiconductor phase $Bi_2Sr_2CuO_y$, a compound of Bi and Ca, etc., were also noted. Figure 1 represents dependence of the zero T_c on the sintering time. It can be seen from the figure that the zero T_c rose after recalcining, and that an optimal value existed for sintering time. Long trailings were also observed in all cases near zero T_c. The SEM picture, in turn, definitely showed that the particle size did not depend on the sintering time, but that the size was reduced by recalcining.

Table 1. Results of Phase Identification by X-Ray Diffraction

Ratio of components	2:2:1:2	2:2:1.5:2.5	2:2:2:3
Before calcination	$Sr(NO_3)_2$ $Ca(NO_3)_2 \cdot nH_2O$ $Cu(NO_3)_2 \cdot nH_2O$	$Sr(NO_3)_2$ $Ca(NO_3)_2 \cdot nH_2O$ $Cu(NO_3)_2 \cdot nH_2O$	$Sr(NO_3)_2$ $Ca(NO_3)_2 \cdot nH_2O$ $Cu(NO_3)_2 \cdot nH_2O$
After calcination	2201, CuO, $SrCO_3$ Bi-Ca compound	2201, CuO, $SrCO_3$ Bi-Ca compound	2201, CuO, $SrCO_3$ Bi-Ca compound
After re-calcination	2201, 2212, CuO Bi-Ca compound	—	2212, 2201, CuO Bi-Ca compound
After sintering	2201, 2212 Bi-Ca compound	2201, 2212 Bi-Ca compound	2201, 2212 Bi-Ca compound

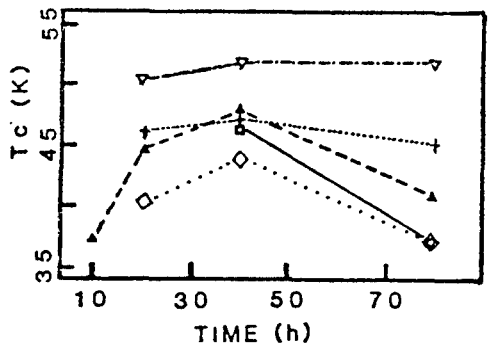

+ 2:2:1:2 (Calcination only) Δ 2:2:1:2 (Recalcination)
□ 2:2:1.5:2.5 (Calcination only) ∇ 2:2:2:3 (Recalcination)
◊ 2:2:2:3 (Calcination only)

Figure 1. Plot of the Zero T_c Vs. the Sintering Time

Synthesis of Ag-Added Bi-Pb-Ca-Cu-O Powder by Spray Drying, Superconductivity of Powder

906C7512 Tokyo SERAMIKKUSU KISO KAGAKU TORONKAI in Japanese 24 Jan 90 p 174

[Article by Hiroko Higuma, Mitsunobu Wakata, Fusaoki Uchikawa, and Kiyoshi Yoshizaki, Zaiken (the Material Laboratory), Mitsubishi Electric Corp., Ltd.)

[Text] **1. Introduction**

This research deals with uniform dispersion of Ag in the powder of Bi(Pb) series of oxide superconductors by the spray-drying method and with the essential effects of the Ag addition on the powder involving limited grain boundary influence.

2. Experiments

A solution of oxides of Bi and Pb, acetates of Sr, Ca, and Cu, and the acetate of Ag in 0.05 mol/ℓ aqueous ethanol was prepared and subjected to spray drying to give a powder and then pyrolyzed and crystallized for 20 hours at 852~855°C such that Ag could be added to the ceramic $Bi_{1.84}Pb_{0.34}Sr_{1.91}Ca_{2.03}Cu_{3.06}O_v$ in the ratio of 0.08 and 0.17 mol of Ag to 2.3 mol of Ca. Effects of the addition of Ag on the crystallization into the high T_c phase was studied by X-ray diffraction and by thermal analysis. The particle size was measured by scanning electron microscope (SEM) observation and by sedimentation, and magnetic properties by superconducting quantum interference device (SQUID) susceptibility, etc. The results were then compared with those for the ceramic with no Ag addition.

3. Results and Discussion

No Ag crystal peaks were noted in the X-ray diffraction pattern of the spray-dried powder, but, following crystallization for 20 hours at 852°C, the powder exhibited two phases, those of the metal Ag and the high T_c (powder A). Thermal analysis showed that Ag had the effect of reducing the melting point of the Bi-Pb series. Reflecting these results, the ceramic powder with no Ag addition and processed at 855°C for 20 hours had the greatest high thermal conductivity content (powder B). Particles of both powders A and B exhibited almost equal crystal growth with nearly identical particle size and shape: 5~10 μm and

plate form. Assuming from the temperature dependence of the magnetic moment, powders A and B underwent transition into the high T_c at approximately 5~50 G. Dependence on the magnetic field intensity of the magnitude of standardized hysteresis, ΔM, from the hysteresis curves of the magnetic moments at 77 K for both powders are shown in the figure. It is seen from the figure that the dependence on magnetic field intensity of ΔM for powder A is smaller than for powder B, which suggests the possibility that addition of Ag to the powder of the Bi-Pb-series of oxide-superconductors reinforces the pinning intensity of the powder.

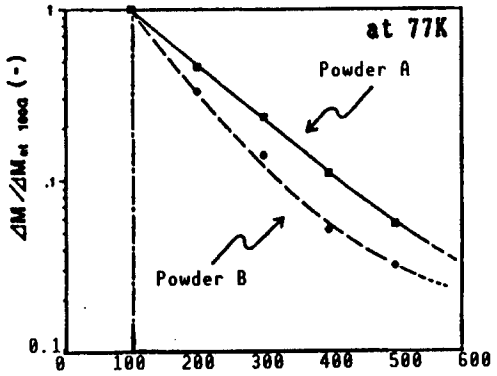

Figure 1. Magnetic Field Dependence of ΔM Normalized by the Value at 100 G

Composition, Superconducting Properties of Y-Ba-Cu-O Film Prepared by CVD

906C7512 Tokyo SERAMIKKUSU KISO KAGAKU TORONKAI in Japanese 24 Jan 90 p 175

[Article by Akira Suhara, Hisanori Yamane, Toshio Hirai, Kinken (IMR), Tohoku University, and Hideyuki Kurosawa, Riken Co., Ltd.]

[Text] **1. Introduction**

Superior superconducting properties for the Y-Ba-Cu-O film prepared by CVD have recently been reported. This research aimed to synthesize the film by CVD on the single-crystal substrates MgO(100) and $SrTiO_3$(100), to study the composition, microstructure, crystalline structure, and superconducting features of the film, and to elucidate the dependence of these properties on substrates.

2. Methods of Experiments

The materials used were the β-diketone metal complexes of Y-thd_3 ("thd" short for 2,2,6,6-tetraethyl-3,5-heptanedionate), Ba-thd_2, and Cu-thd_2, which were synthesized with a hot-wall-type CVD oven. Films of various compositions were prepared by varying the temperature for vaporizing the material in the range from 110~275°C. The vaporized materials were carried to the substrate by argon gas; oxygen gas was introduced by another route; the internal pressure was kept at 10 torr and deposition temperature at 850°C. Following the deposition reaction, the introduction of argon gas was stopped and an in-situ oxygen treatment carried out whereby the oven temperature was brought down to room temperature at a rate of 15°C/minute under an oxygen atmosphere of 1 atm. The resultant film was then subjected to analysis by X-ray diffraction, to scanning electron microscope (SEM) observation, to measurement of T_c and J_c, and, further, to analysis of its composition for Y, Ba, and Cu by means of ICP emission spectrometry.

3. Results

Figure 1 presents plots of the composition of the film vs. the T_c. Of the films produced on the $SrTiO_3$ substrate, those with the ratio of Y, Ba, and Cu around 1:2:3, or those involving greater proportions for Cu than that, had a T_c of 87~92 K. The films produced on the MgO substrate, in turn, had a T_c of

80~89 K in the identical composition region. Whereas the $SrTiO_3$ substrate afforded the film a J_c value of about $10^5 A/cm^2$, the one on the MgO substrate had a maximum J_c value of only $10^3 A/cm^2$. The microstructure with high T_c and high J_c values presented a picture of insularly scattered CuO in a compact matrix. The X-ray diffraction picture also showed that the film was predominantly oriented in the direction of the c axis with scattered grains oriented in the direction of the a axis.

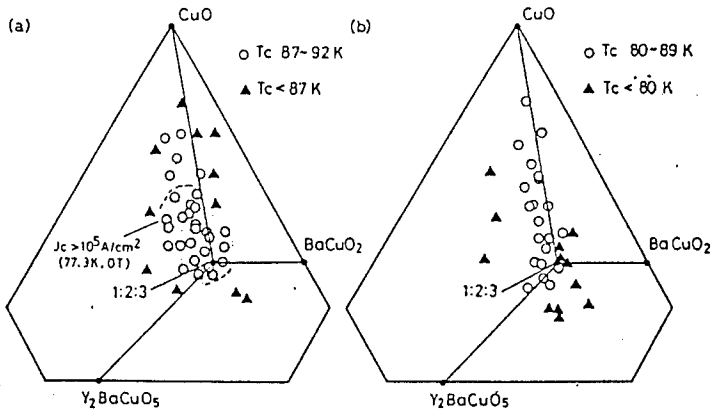

Figure 1. Relationship Between Film Composition and T_c (T_{dep}: 850°C)
(a) $SrTiO_3$(100); (b) MgO(100)

Microstructure, Properties of High-Temperature Bi Superconducting Ceramics

906C7512 Tokyo SERAMIKKUSU KISO KAGAKU TORONKAI in Japanese 24 Jan 90 p 177

[Article by Toshihiko Nishida, Takashi Otsuka, Susumu Shimano, Takeshi Shiono, and Tomozou Nishikawa, Department of Industrial Arts, Kyoto Institute of Technology]

[Text] **1. Introduction**

The authors have shown that it is possible to produce superconducting wires of high density by sealing powders or sintered compacts of the relevant ceramics into metal molds and then, after having preheated them for a short time, by subjecting them to an extrusion at high temperatures.[1,2] Nevertheless, some improvements in the material and design of the metal mold seem to be necessary since many of the ceramics exhibiting superconductivity at high temperatures are crystallographically unstable and their crystal phases, hence, are liable to be transformed in the process of molding. This report deals with an investigation of the possibility of molding at high temperature of the material $Bi_{1.8}Pb_{0.4}Sr_2Ca_2Cu_{3.2}O_x$ (2223 phase) and with superconducting properties of the resultant ceramics.

2. Experiments and Results

The powder of $Bi_{1.8}Pb_{0.4}Sr_2Ca_2Cu_{3.2}O_x$ (involving some $Bi_2Sr_2CaCu_2O_x$) prepared by a solid phase reaction was sealed into metal molds and, after having been preheated at 820°C, was immediately subjected to extrusion or compression molding. Both the extrusion and compression molding allowed a smooth change in shape and produced scarce cracks within the ceramics. Figure 1 represents X-ray diffraction of the powder before and after molding; (a) represents before molding; (b) after molding with use of a Cu mold; and (c) after molding with use of a mold of Ni lined with Ag. Figure 2 represents the dependence on temperature of the electrical resistance of: (a) the powder molds, and (b) and (c) the compacts processed at high temperatures. Results of X-ray diffraction analysis exhibited few crystallographic changes before and after the molding, but the superconducting feature was exhibited in different manners, suggesting that the material of the mold and other conditions, such as temperatures and pressures, in molding were of extreme importance for the superconductive property of the wire material.

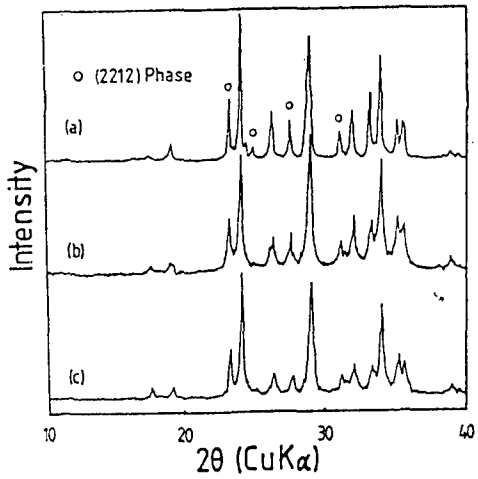

Figure 1. Powder X-Ray Diffraction Pattern Before and After High-Temperature Processing

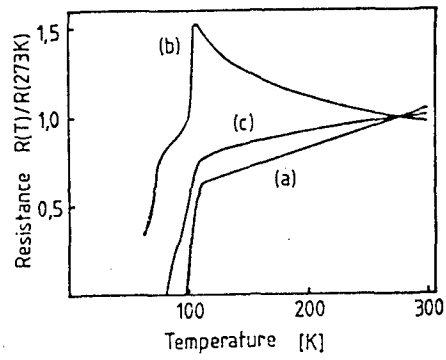

Figure 2. Superconductivity Characteristics

References

1. Nishida, Shiono, Otsuka, and Nishikawa, POWDER AND POWDER METALLURGY, Vol 34, 1987, p 465.

2. Ibid., Vol 36, 1989, p 468.

Addition of Silver Into Superconducting Oxide Ceramics

906C7512 Tokyo SERAMIKKUSU KISO KAGAKU TORONKAI in Japanese 24 Jan 90 p 184

[Article by Yasumichi Matsumoto, Yoshiaki Yamaguchi, and Jukichi Honbo, Faculty of Engineering, Kumamoto University]

[Text] **1. Objective**

It has been reported by the authors' laboratory and other research organizations that the addition of silver to superconducting oxide ceramics allows an increase in J_c, a slight increase in T_c, enhancement of crystal growth of the grains of superconductors, etc., which contribute substantially to practical applications of the material. All relevant research is in agreement that the silver acts on the grain boundary in an important manner in displaying these effects and, particularly, in improving the value of J_c, but it has yet to be definitely shown whether the effects result from an enhancement of the sintering of the grain boundary or from the presence of the metal, which produces the so-called infiltrating effects. In the former case, the mechanism involved in the enhancement of sintering effect still remains controversial. Assuming that the improved J_c value was accomplished by the former and that the silver ions diffused into the grain boundary and enhanced sintering of the site, as the authors believe, we conducted an investigation to prove these assumptions and to determine the role played by the silver in enhancement of sintering at low temperatures.

2. Experiment

To the powder of $YBa_2Cu_3O_y$ prepared by the powder method were added a number of silver compounds, and the mixture was sintered at different temperatures ranging from 400~930°C. The compact was measured for its R-T curve by the four-terminal methods observed for sintered states by scanning electron microscope (SEM), etc., and measured for the decomposition temperatures of individual silver compounds from the TG-DTA curve.

3. Results

Figure 1 presents R-T curves for $YBa_2Cu_3O_y$. All specimens of the compact having an added Ag compound exhibited a rise in electric conductivity, except for

silver acetate, even in a compound of ionic bonding, AgCl, in comparison with the one with no Ag added, and displayed a definite critical temperature at about 90 K although perfect zero resistance was not reached. Where no Ag was added, no definite critical temperature was present. The lack of a definite critical temperature in the R-T curve in this case results from the presence of a liquid phase that surrounds the superconductor particles and that prevents satisfactory sintering and binding of these particles. It is evident that Ag compounds help accomplish the sintering. It is also evident that it is not the metal Ag, but ions of Ag (possibly Ag^+) that help this sintering, since the effect is still observed in spite of the absence of the decomposition of AgCl into the metal Ag.

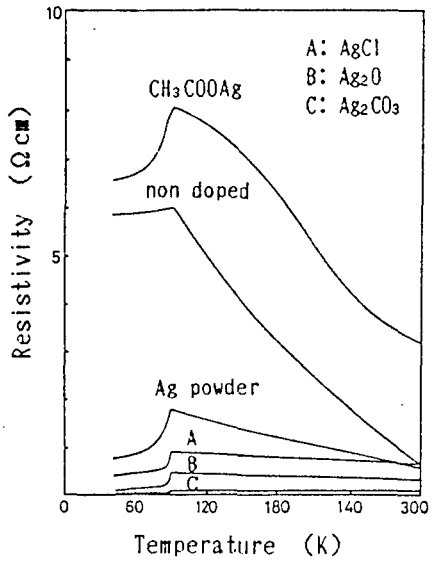

Figure 1. Plots or Resistivity Vs. Temperature for $YBa_2Cu_3O_y$ to Which Different Silver Compounds Have Been Added (700°C 10-hour sintering)

Determination of Oxygen Content of $YBa_2Cu_3O_{7-y}$ Superconductors

906C7512 Tokyo SERAMIKKUSU KISO KAGAKU TORONKAI in Japanese 24 Jan 90 p 185

[Article by Yoko Suyama, Mamoru Matsumoto, and Toshitaka Hayakawa, Japan Fine Ceramics Center]

[Text] **1. Objective**

Superconducting characteristics of the oxide superconductors of the yttrium series are intimately related to oxygen defects. The present investigation deals with the qualitative estimation of oxygen content of the superconductors $YBa_2Cu_3O_{7-y}$ with high precision and with a study of the relationship between the lattice parameters and the oxygen defects.

2. Method of Experiments

From the materials Y_2O_3, $BaCO_3$, and CuO, all with a purity of 99.99 percent, sintered compacts $YBa_2Cu_3O_{7-y}$ of three types with different molar ratios for oxygen were prepared, and a quantitative analysis of the compositions of these compacts carried out; namely, Y, Ba, and Cu were analyzed by wet chemical analysis and trace impurities by ICP emission spectrometry, carbon analyzer, etc.; oxygen was estimated quantitatively by an oxygen analyzer based on the method of inert-gas fusion infrared absorption; critical temperatures and critical current densities were measured by four-terminal method, and crystal phases and lattice parameters by X-ray diffraction.

3. Results and Discussion

Table 1 presents results of the analysis of the compositions. The ratio of Y, Ba, and Cu were 1:2.02:3.01. Analysis of the measurement conditions showed that the value of the oxygen was reliable up to four digits, as seen in the table, and the standard deviation of the value at 0.07 allowed precise enough measurements. The values of the oxygen obtained by the present method must be of higher precision and accuracy than those from the conventional TG method or chemical analysis used for determination of oxygen of superconductors. The molar ratio of oxygen for the specimens A, B, and C decreased in that order, namely 6.864, 6.520, and 6.220, respectively. The contaminant metals demonstrated were Fe, Ca, Sr, and Si, totaling about 0.01 percent; the other

elements involved were 0.06~0.10 percent by weight of C and 0.02~0.10 percent by weight of H_2O. The T_c(on) of specimens, A, B, and C fell with falling oxygen content, that is, 93.8 K, 60.6 K, and below 14 K for A, B, and C, respectively. The relationship between the values of oxygen defect estimated as above and those of the lattice parameters obtained by the (Leetbelt) analysis of X-ray diffraction data is presented in Figure 1.

Table 1. Compositions of Superconductors of YBCO Series

(Unit: wt%)

Component / Specimens	Major components			
	Y	Ba	Cu	O
A	13.26 (1.000)	41.45 (2.024)	28.57 (3.015)	16.38 (6.864)
B	13.38 (1.000)	41.83 (2.024)	28.78 (3.009)	15.70 (6.520)
C	13.50 (1.000)	42.16 (2.022)	29.05 (3.011)	15.11 (6.220)

(The figures in ( ) represent molar ratios based on Y as 100)

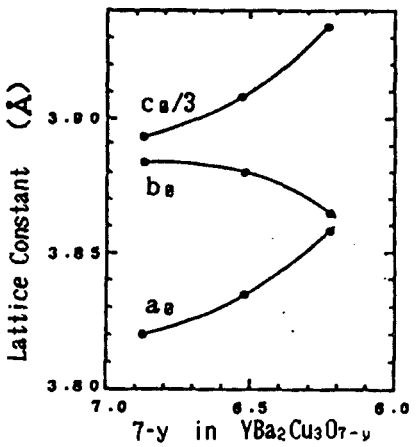

Figure 1. Plots of Oxygen Contents Vs. the Lattice Parameters

Synthesis of Mullite From SiO_2 Powders-Al Salt Solutions

906C7512 Tokyo SERAMIKKUSU KISO KAGAKU TORONKAI in Japanese 24 Jan 90 p 195

[Article by Hiroyuki Nakamura, Yukiko Katae, and Akio Kato, Engineering Department, Kyushu University]

[Text] **1. Introduction**

Mullite, $3Al_2O_3 \cdot 2SiO_2$, has the prospect of application in high-temperature structures and, by use of inorganic salts as the raw materials, the material may be afforded at lower costs, although the alkoxide method has been subjected to research more frequently. The present research deals with a method wherein the Al_2O_3 component in an amount corresponding to that in the mullite composition was precipitated on a colloidal silica in an aqueous aluminum salt solution in which the silica had been dispersed by a homogeneous precipitation method involving the use of urea.

2. Method of Experiments

SiO_2 sol, with particle diameters from 0.008~0.02 μm, was dispersed in distilled water and then an Al salt dissolved therein. After the solution reached a given temperature, urea was added to start the reaction. The quantity of CO_2 liberated and the pH of the solution were followed through the course of the reaction. The resulting precipitate was washed by the centrifuge method and dried in vacuum at 70°C; the powder yielded was treated thermally and then checked for the formation of mullite. The thermally treated product was further subjected to sintering.

3. Results

The powder produced was in the gel state when $Al(NO_3)_3$ or $AlCl_3$ was involved as a raw material, but in particle state in the case of $Al_2(SO_4)_3$. In the former case, the powder did not yield the single mullite phase after heating at 1,300°C for 3 hours; in the latter case, however, where a reaction involving urea concentrations of 0.9, 1.8, or 3.6 mol/ℓ, reaction temperatures of 80, 90, or 95°C, and $Al_2(SO_4)_3$ concentrations of 0.0375, 0.075, or 0.15 mol/ℓ was carried out to give a powder, the single mullite phase was yielded by heating at 1,250°C for 1 hour. Figure 1 presents a scanning electron

microscope (SEM) picture of the powder involving $Al_2(SO_4)_3$ having been subjected to the thermal treatment. Al_2O_3 component was found amorphous at pH 7, but turned into a boehmite-like crystal at pH 8 or above, which did not turn into the single mullite phase after the thermal treatment even for 3 hours and at 1,300°C. The powder having been turned into the single mullite phase was investigated for its sintering properties. The results are presented in Table 1. As can be seen, sintering for 3 hours at 1,600°C yielded a sintered compact with a relative density of 96 percent.

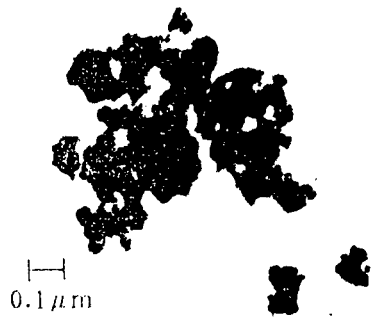

$Al_2(SO_4)_3$ concentration: 0.075 mol/ℓ
SiO_2 concentration : 0.05 mol/ℓ
SiO_2 grain diameter : 0.008 μm
Urea concentration : 1.8 mol/ℓ
Reaction temperature : 90°C
Values of pH at time the reaction stopped : 7.2
Heating conditions : 1,250°C, 1 hour

Figure 1. Thermally Treated Objects

Table 1. Properties of Sintered Compact (Sintering time of 3 hours)

	1,550°C	1,600°C
Relative density (%)	82.4	96.0
Ratio of closed pores (%)	0.9	4.0
Ratio of open pores (%)	16.7	0

Preparation of γ-Alumina Thin Porous Membrane by Sol-Gel Method

906C7512 Tokyo SERAMIKKUSU KISO KAGAKU TORONKAI in Japanese 24 Jan 90 p 196

[Article by Tatsuya Okubo, Masayuki Watanabe, Katsuki Kusakabe, and Shigeharu Moroka, Engineering Department, Kyushu University]

[Text] Aluminum isopropoxide was subjected to hydrolysis with a large quantity of distilled water and then dispersed with hydrochloric acid to give a stable "colloidal sol" of boehmite, γ-AlOOH. An alumina perforated pipe with thin perforations of 1.1 μm in diameter, after having its external surface coated with a film of polyvinylidene chloride, was dipped in the sol for 10 seconds, such that a thin film was formed over the internal surface, then dried in air, and sintered at 773 K (50 K/h) to give γ-alumina.

Preparation of a γ-alumina thin film free of pinholes was successfully accomplished by repeating twice the procedure of dipping in the sol, drying, and sintering. Figure 1 presents a scanning electron microscope (SEM) picture of the internal part of the pipes as scanned obliquely from above; the relevant film thickness was about 5 μm. The pore structure of the film before and after the sintering was observed further with an SEM of high resolution, as shown in Figure 2. Also shown was the same picture for a film prepared from polymeric sol—a sol prepared by hydrolysis of a solution of the alkoxide in 2-propanol-triethanol amine—where the films were not free of pinholes. The film made from the colloidal sol showed that it was made up of rod-shaped particles in lamination, that the structure of pores did not change by sintering, and that the pore diameter was uniform at about 5 nm. The film prepared from the polymeric sol, in turn, was made up of spherical particles, and its microstructure suffered major changes depending on the method of preparation of the sol.

Table 1 presents sizes of particles constituting the film prepared from the colloidal sol. Agreement of the value estimated by XRD with those obtained by the other method showed that the rod-shaped particles in Figure 2 corresponded to the single-crystal of the material.

Permeation characteristics for N_2 and He gases of film prepared from colloidal sol were estimated. The rate of permeation of the film after the substrate had been removed followed the Knudsen rule and proved that the thin film was free from pinholes and that it had pores controlled uniformly in fine size.

Table 1. Grain Diameters Estimated by Different Methods

	Boehmite	γ-Alumina
BET method[1]	D_{sphere} = 3.8 nm	D_{sphere} = 5.6 nm
X-ray diffraction[2]	D_{120} = 3.8 nm	D_{440} = 3.4 nm
Scanning electron microscopy (SEM)	(Not clear)	ϕ4 nm x 25 nm
Dynamic light scattering	D_{Stokes} = 12 nm	(Not applicable)

Figure 1. SEM Picture of Internal Surface of Pipe Wall

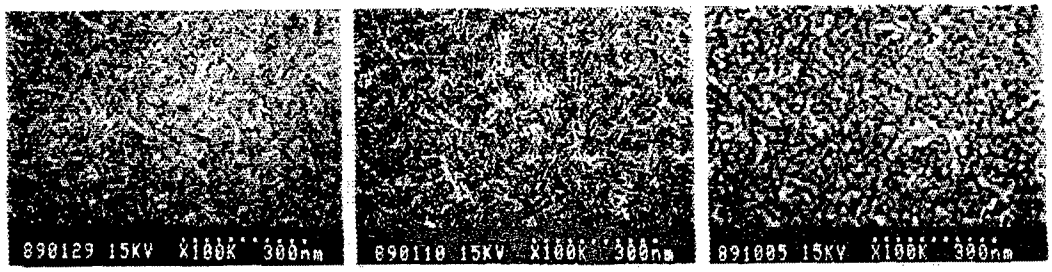

Prior to sintering for the colloidal sol

After sintering for the colloidal sol

After sintering for the polymeric sol

Figure 2. High-Resolution SEM Picture of the Surface of Films

Preparation of $LiTi_2(PO_4)_3$ by Sol-Gel Method

906C7512 Tokyo SERAMIKKUSU KISO KAGAKU TORONKAI in Japanese 24 Jan 90 p 197

[Article by Noboru Toge, Jishun Zhu, and Tsutomu Minami, Department of Applied Chemistry, University of Osaka Prefecture]

[Text] **1. Objective**

The ceramic $Li_{1+x}M_xTi_{2-x}(PO_4)_3$, where M is Al, Sc, Y, or La, has recently been reported to have a high lithium ion conductivity of 10^{-4}S/cm or above at room temperature and to make a prospective material of the stable lithium ion conductor.[1] The material powders for such ion-conductor ceramics have generally been prepared by a solid phase reaction, which, nevertheless, are not capable of affording required uniform powders readily. The present research is aimed at preparing material powders for sintering by the sol gel method using metal alkoxides as the starting material and deals with conditions for the synthesis of $LiTi_2(PO_4)_3$ (x = 0).

2. Methods of Experiment

Figure 1 presents the procedure for preparing the gel $LiTi_2(PO_4)_3$. Metal Li was first allowed to react with methanol, and titanium tetrabutoxide, $Ti(OBu)_4$, diluted in ethanol, was then added in the Li-to-Ti ratio of 0.5. The resulting solution was subjected to refluxing at 80°C for 24 hours. Triethyl-phosphate, $Po(OEt)_3$, was next added at room temperature in the P-to-Ti ratio of 3, stirred for 2 hours, and an aqueous ethanol added slowly to allow hydrolysis of the material. The solution was allowed to stand for several days at 50°C to give a uniform gel solution, which was then dried and thermally treated at various temperatures such that the relationship between the process of deposition of $LiTi_2(PO_4)_3$ and the condition for preparing the gel could be elucidated.

3. Results and Discussion

Preparation of the gel was attempted in various ways, but all except the one presented in Figure 1 failed to give the gel readily. A TG-DTA measurement of the dried gel obtained by the procedure of Figure 1 showed a peak of heat emission in the vicinity of 315°C, resulting from combustion of residual organic matters. The specimens treated thermally at 350°C for 10 hours was

amorphous, as seen in Figure 2(b). A thermal treatment allowed anatase to begin depositing at 600°C or above and $LiTi_2(PO_4)_3$ together with rutile at about 900°C. The specimens treated for 24 hours at 1,000°C showed a picture of peaks of predominantly the intended $LiTi_2(PO_4)_3$, but some peaks of rutile and a few unidentified peaks were also present. With the amount of deposition of rutile depending largely on the condition under which the gel is formed, it may conceivably be possible to reduce the amount by optimizing the condition for the gel formation and the thermal treatment. Sintering properties of these powder specimens will also be reported in the coming meeting.

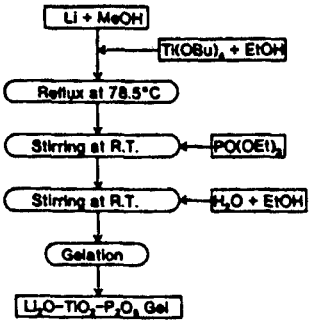

Figure 1. Production Procedure

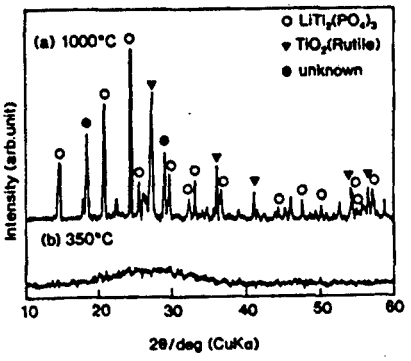

Figure 2. X-ray Diffraction Pattern

References

1. Aono, H., et al., J. ELECTROCHEM. SOC., Vol 136, 1989, p 590.

Preparation of $ZrSiO_4$ Powder by Using Sol-Gel Method--Part 2

906C7512 Tokyo SERAMIKKUSU KISO KAGAKU TORONKAI in Japanese 24 Jan 90 p 198

[Article by Toshihiro Terazaki, Hidehiko Kobayashi, and Takashi Mitamura, Engineering Department, Saitama University, and Toshiyuki Mori and Hiroshi Yamamura, Tosoh Co., Ltd.: "Part 2: Effect of the Rate of Rise and Fall of Temperature and Addition of Seed Nuclei"]

[Text] **1. Introduction**

Zircon, $ZrSiO_4$, represents an oxide composite with mechanical properties similar to those of mullite, $3Al_2O_3 \cdot 2SiO_2$. The zircon powder that has been available to date has been prepared from natural zircon sand and involved various contaminants, which enhances thermal dissociation and deteriorates superior properties of the oxide composite, thus preventing the unique properties from being elicited satisfactorily. The present research is aimed at producing zircon of high purity and deals with the effects of the rate of the rise and fall of the temperature and the addition of zircon crystal seeds for various sintering temperatures on the relevant specimens prepared by application of the coprecipitation method for zirconia sol and silica sol.

2. Method of Experiment

The starting materials used were zirconia sol (made by Nissan Chemicals Co., Ltd., NZS-20A) and silica sol (made by Nissan Chemical Co.: SNOWTEX-O). The pH of a solution containing the two materials in equimolar composition was adjusted and set at the isoelectric point, followed by the coprecipitation of the solution and gel formation. The aqueous component of the gel was removed by an evaporator to give dried gel, which was calcined for 3 hours at 700°C to give a powder with the composition of zircon. Finally, a commercially available zircon powder (made by Koujundo Kogaku Co., Ltd., purity 98%) was added to the prepared powder in the range of 0~1.5 percent as the seed crystal; the resultant mixture of powder was subjected to sintering for 2 hours at 1,200~1,600°C to yield the intended powder. The rate of the rise and fall of the sintering temperature, at this juncture, was varied in the range of 0.15~10 K/minute. The specimens so produced under different sintering conditions were then identified by X-ray diffraction tests; the amount of zircon produced was estimated by using four peaks of the monoclinic form and

tetragonal form of zirconia and zircon present at 2 θ of 26~32° in the X-ray diffraction pattern.

3. Results and Discussion

Figure 1 presents the effects of the heating rate in sintering and the addition of zircon crystal seeds (1.5 percent by weight added in the figure) on the zircon content. Where the sintering temperature was below 1,300°C, the effect of the rise and fall of the temperature as well as that of the addition of the seed crystals were pronounced. These results demonstrated that, where the sintering temperature was below 1,300°C, reduction of the heating rate and addition of seed crystals jointly served to enhance the content of zircon, and that, for sintering temperatures above 1,400°C, addition of crystal seeds acts more than heating-rate change to help to increase the content. Addition of zircon seed crystals in 0.25~1.0 percent by weight was satisfactory in the experimental range.

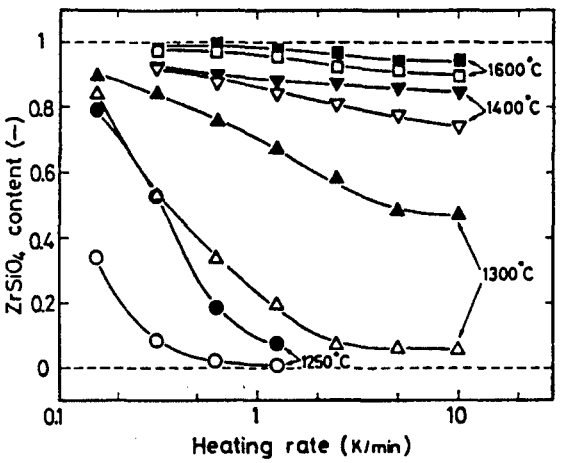

Figure 1. Effect of Heating Rate and Addition of Commercial Zircon Powder on Synthesis of Zircon
o: Nonaddition; •: 1.5 percent by weight

Preparation, Crystallization of System SiO_2-TiO_2 Through Alkoxide Processes

906C7512 Tokyo SERAMIKKUSU KISO KAGAKU TORONKAI in Japanese 24 Jan 90 p 199

[Article by Shoji Kaneko and Satoshi Suzuki, Shizuoka University]

[Text] **1. Introduction**

The high-temperature characteristics of silica may conceivably be improved by converting it to a solid solution with titania, which is hard to accomplish because of the anatase that continues to be present even at temperatures above 1,400°C.[1,2] The present investigation is aimed, in connection with the composition of this silica rich system, at producing a more uniform gel by using metal alkoxides as the raw material and by application of urea and thus at eliminating the anatase. Therefore, it deals with the solid solution state of the system and the limit to the solid-solution for titania.

2. Method of Experiment

Ethyl orthosilicate and titanium isopropoxide were mixed in a given proportion (metal-ion concentration of 0.4 $mol \cdot dm^{-3}$) and, following addition of methanol and urea, the mixture was heated at 80°C to provide a gel. The gel was dried for 24 hours at 110°C, calcined for 2 hours at 800°C, molded, and again thermally treated at a higher temperature. Fluorescence X-ray was used for measurement of total titania, and powder X-ray diffraction for measurement of lattice parameters and for quantitative analysis of the quantity of the solid solution. Measurement was also taken for the temperature of transition from α to β phase of cristobalite by means of differential thermal analysis.

3. Results and Discussion

The gel was prepared and thermally treated after adding HCl or ammonia water, and relevant effects on the transformation from anatase to rutile was investigated. For the specimens of the gel prepared and thermally treated after addition of small amounts of ammonia water, anatase was not detected and all excess titania being present as rutile. This may conceivably result from the rates of the decomposition of the two alkoxides approaching equivalent and hence forming of more uniform gel.

For the specimens thermally treated for 48 hours at 1,400°C and with a titania content of 2~10 percent by weight, the lattice constants rose with increasing titania content and then stayed stationary after the content reached 4~5 percent. This suggests that formation of solid solution reached its maximum limit there and that the real limit is 1.3 percent by weight by subtracting the excess titania present as rutile, as referred to above. The temperature for α and β phase transition proved to fall with rising titania content and then also remained stationary after the content reached 4~5 percent. The change was in agreement with that of the lattice parameters and suggested that the relevant transition temperature fell with rising content of titania in solid solution. For the thermal treatment temperature of 1,450°C and 1,500°C, the relevant limit proved to be 1.6 and 2.0 percent by weight, respectively, suggesting increasing value of the limit with rising thermal-treatment temperature. A high-temperature phase diagram for SiO_2–TiO_2 partially revised on the basis of these values is presented.

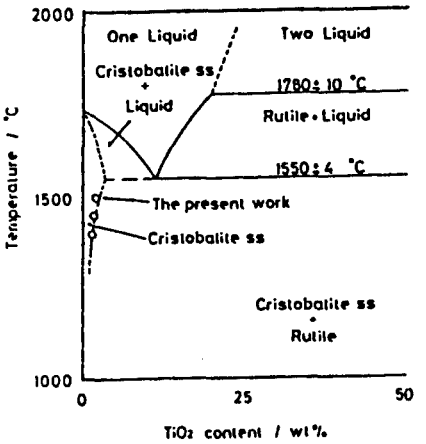

Figure 2. Partial Phase Diagram of the System SiO_2–TiO_2 Proposed Tentatively on the Basis of Present Work

References

1. Kaneko, S., et al., CERAMURGIA INT'L., Vol 6, 1980, p 106.

2. Kaneko, et al., Preliminary manuscript for the 27th Forum of the Basic Science of Ceramics, 1989, p 2.

Properties of Titanium Oxide Formed by Hydrolysis of Titanium Alkoxide

906C7512 Tokyo SERAMIKKUSU KISO KAGAKU TORONKAI in Japanese 24 Jan 90 p 200

[Article by Tadashi Sasamoto, Sumie Enomoto, Zenya Shimoda, and Yuzo Saeki, Kanagawa Institute of Technology]

[Text] **1. Introduction**

The present research deals with changes in crystalline structure by heating of the hydrolysis product obtained from tetraisopropyl orthotitanate and the effects of conditions of the relevant hydrolysis on those changes, as part of the investigation into the properties of the titanium oxides produced by the hydrolysis of titanium alkoxides.

2. Experiment

Ten grams of $Ti(O-i-C_3H_7)_4$, either diluted with alcohol or not diluted with any material, were hydrolyzed by adding 5, 10, and 20 times in molar ratio of water. The hydrolyzed materials were then subjected to thermal analysis in the temperature range from room temperature to 900°C; materials obtained by heating the above product for 2 hours at different temperatures were examined by X-ray analysis. Subsequently, the above alkoxide was hydrolyzed by adding any of 3 percent by weight of H_2SO_4, HNO_3, or HCl, 1 percent by weight, of HNO_3, and 7 percent by weight of HNO_3 instead of pure water, and the resultant products were examined in the same manner.

3. Results

Table 1 presents the changes in crystalline structure of the material, which had been obtained by hydrolyzing the above nondiluted alkoxide with unadulterated water, after heating, for 2 hours at different temperatures. The product obtained from the alkoxide diluted with alcohol and subjected to hydrolysis with unadulterated water gave nearly identical results.

Where the alkoxide was hydrolyzed with 3 percent by weight of H_2SO_4, the crystallization from the amorphous state to anatase and the thermal transformation from anatase to rutile were all suppressed as compared with the case where the alkoxide was hydrolyzed with pure water, whereas, in the case of

hydrolysis with HCl and HNO_3 in contrast, thermal transformation from anatase to rutile was accelerated (Table 2). In the latter case, effects of enhancement of the relevant changes were pronounced when the acid in 20 times in molar ratio was used for hydrolysis, and, in particular, an extreme enhancement in the production of rutile was noted by hydrolysis with use of 7 percent by weight of HNO_3 in 20 times in molar ratio.

Table 1. Amount of H_2O Added to $Ti(OC_3H_7)_4$ in Molar Ratio

Heating temperature (°C)	Amount of H_2O added to $Ti(OC_3H_7)_4$ in molar ratio		
	5 times amount	10 times amount	20 times amount
No heat addition	amor	amor	amor
100	A	A	A
200	—	—	—
300	—	—	—
400	—	—	—
500	A	A	A
600	R>A	R>A	R>A
700	R>>A	R	R>>A
800	R	—	R

amor: amorphous; A: anatase; R: rutile

Table 2. Amount of 3 Percent HNO_3 Added to $Ti(OC_3H_7)_4$ in Molar Ratio

Heating temperature (°C)	Amount of 3 percent HNO_3 added to $Ti(OC_3H_7)_4$ in molar ratio		
	5 times amount	10 times amount	20 times amount
No heat addition	amor	amor	amor
100	A	A	A
200	—	—	A>R
300	—	A	A≈R
400	A	A>R	R>>A
500	A>R	R>>A	R
600	R	R	—

amor: amorphous; A: anatase; R: rutile

Preparation of Porous Silica Glass by Sol-Gel Method

906C7512 Tokyo SERAMIKKUSU KISO KAGAKU TORONKAI in Japanese 24 Jan 90 p 204

[Article by Hiromitsu Kozuka, Jun Yamaguchi, and Sumio Sakka, Institute for Chemical Research, Kyoto University]

[Text] **1. Introduction**

The authors suggested a high-hydrochloric acid sol gel method, featuring use of a large quantity of hydrochloric acid and a small quantity of water, as a method for synthesizing silica monoliths that are free of cracks.[1] In this method, the size of the particles constituting the skeleton of the gel is allowed to grow up to a maximum of 5 μm by increasing the quantity of HCl. The present research evaluates the porous characteristics of the relevant gel compact for studying the possibility of the compact as a precursor of porous silica glass.

2. Experiment

From the materials TMOS, H_2O, HCl, and CH_3OH in the molar ratio 1:1.53:0.15~0.40:2 was prepared 50 mℓ of an alkoxide solution that was allowed to stand at 40°C in a 120-mℓ polypropylene container. After allowing the process of gel formation and aging of the solution to go on for 24 hours in an open or sealed condition, the gel was dried at 40°C for 7 days. The dried gel subsequently had its temperature raised at a constant rate up to 800~1,300°C and was kept at that temperature for a given period to give the test specimens, which were assessed for pore characteristics by mercury-pressure (or injection) process.

3. Result

The porous glass produced by thermal treatment for 3 hours at 1,000°C of gels which, in turn, had been yielded from solutions with HCl-to-TMOS ratios of 0.15 and 0.25, exhibited pore-diameter distributions as shown in Figure 1, with medians at 18 nm and 120 nm for the HCl-to-TMOS ratios, respectively. It is evident that the pore size of the glass increased with increasing quantity of HCl acid. In the case of porous bodies produced from additional solutions with the relevant ratio of 0.25, a change of the final temperature of the thermal treatment from 800~1,000°C resulted in a decrease in the volume of

pores from 0.78 cm^3 per g to 0.67 cm^3 per g, and in the median of the pore-diameter distribution from 75 nm to 25 nm, as seen in Figure 2. The possibility of producing silica glasses with different bore characteristics by varying the quantity of HCl in the starting solution and thermal treatment conditions of the gels were thus demonstrated.

The authors here express their gratitude to Professor Masahiko Nakamura of Kyoto Institute of Technology for the guidance and help extended to them in connection with the mercury injection method.

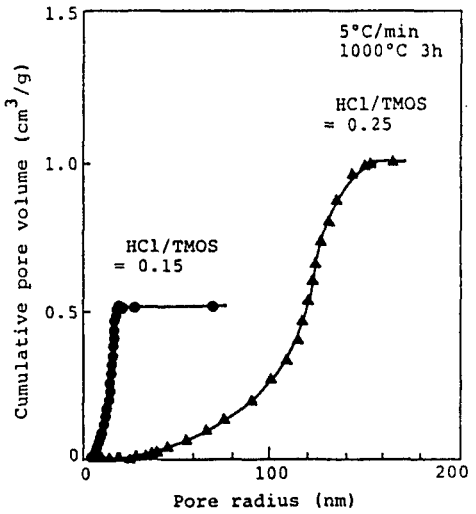

Figure 1. Cumulative Porosity of the Porous Silica Derived From the Solutions of HCl/TMOS = 0.15 and 0.25 by Heating the Gels at a Rate of 5°C to 1,000°C and Keeping for 3 h. The solutions were kept at 40°C for 24 h in closed system for gelation and aging and dried at 40°C for 7 days in open system.

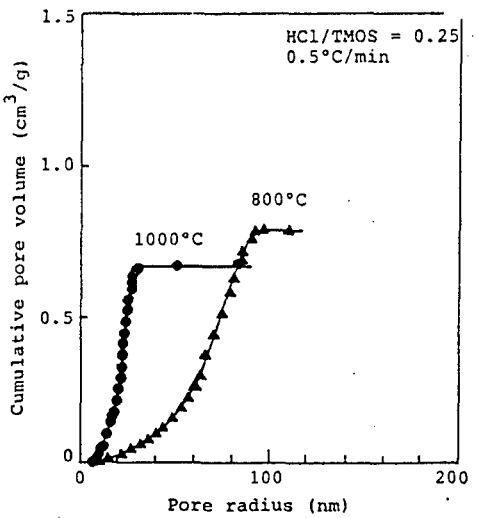

Figure 2. Cumulative Porosity of the Porous Silica Derived From the Solution of HCl/TMOS = 0.25 by Heating the Gel at a Rate of 0.5°C/min to 800 or 1,000°C. The solutions were gelled, aged, and dried at 40°C for 7 days in open system.

References

1. Kozuka, H. and Sakka, S., CHEMISTRY OF MATERIALS, Vol 1, 1989, p 398.

Synthesis of Al_2O_3-ZrO_2 Fibers With Organometallic Precursors

906C7512 Tokyo SERAMIKKUSU KISO KAGAKU TORONKAI in Japanese 24 Jan 90 p 206

[Article by Satoshi Kodama, Toshinobu Yogo, and Hiroyasu Iwahara, Faculty of Engineering, Nagoya University]

[Text] **1. Introduction**

The ceramic of ZrO_2-reinforced Al_2O_3 (ZTA) represents a structural material based on a martensite transformation of ZrO_2 in Al_2O_3, as has been demonstrated, serves to improve the fracture toughness of the material. The ceramic in fiber form also has the prospect of application in heat-resistant materials and composite materials. The present investigation deals with the synthesis of an Al_2O_3-ZrO_2 precursor from an organometallic compound, with subsequent spinning and sintering of the precursor to give the fiber of Al_2O_3-ZrO_2, and with the relationship between the condition for the synthesis of the fiber and the viscosity and roping of the fiber.

2. Method of Experiment

A chelate compound of aluminum and a chelate compound or an alkoxide of zirconium were mixed in a given proportion and, following addition of acetic acid, the mixture was subjected to heat treatment at 150°C. The resulting solution was distilled under reduced pressure such that the low boiling component was eliminated and a desired organometallic-compound precursor was yielded. The precursor was subjected to analysis by IR, NMR, DTA-TG, use of the rotating viscometer, etc. The precursor was sintered in air, and the product analyzed by XRD and transmission electron microscope (TEM). The precursor fiber was prepared by manually plunging a glass rod into the bulk and then drawing it out, or by extrusion of the powder. The fiber was analyzed by scanning electron microscope (SEM) and by micro-Raman spectrometry.

3. Results and Discussion

The alumino metal oxide precursor prepared as above and then subjected to heating in air at 500°C proved to be an amorphous material by XRD identification. Specimens involving different Al-to-Zr ratios and having been subjected to thermal treatment at 1,300°C were identified with respect to the crystal

phase produced, as shown in Figure 1. Where the Zr content in the precursor was 20 at% by weight or less, the ZrO_2 dispersed in the Al_2O_3 was tetragonal crystals. Measurement of the viscosity of the precursor, in turn, proved that the viscosity rose with increasing amounts of acetic acid added and fell with rising measurement-temperature. The precursor proved to be subject to spinning at a certain temperature as a result of an investigation of its capacity for roping for different temperatures. The Al_2O_3-ZrO_2 fiber obtained by sintering the precursor fiber for 1 hour at 1,000°C is presented in Figure 2.

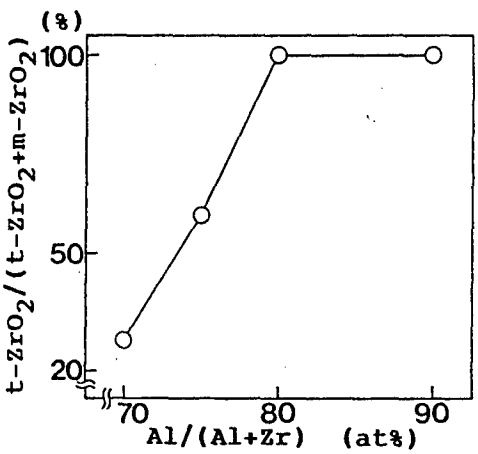

Figure 1. Relationship Between Zr Content and Amount of Produced ZrO_2

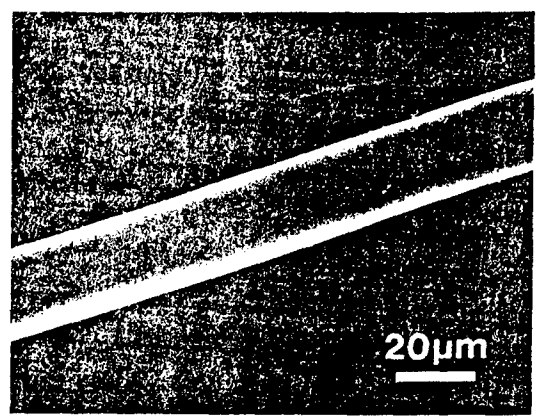

Figure 2. Al_2O_3-ZrO_2 Fiber

- END -

Foreign Broadcast Information Service (FBIS) and Joint Publications Research Service (JPRS) publications contain political, military, economic, environmental, and sociological news, commentary, and other information, as well as scientific and technical data and reports. All information has been obtained from foreign radio and television broadcasts, news agency transmissions, newspapers, books, and periodicals. Items generally are processed from the first or best available sources. It should not be inferred that they have been disseminated only in the medium, in the language, or to the area indicated. Items from foreign language sources are translated; those from English-language sources are transcribed. Except for excluding certain diacritics, FBIS renders personal and place-names in accordance with the romanization systems approved for U.S. Government publications by the U.S. Board of Geographic Names.

Headlines, editorial reports, and material enclosed in brackets [ ] are supplied by FBIS/JPRS. Processing indicators such as [Text] or [Excerpts] in the first line of each item indicate how the information was processed from the original. Unfamiliar names rendered phonetically are enclosed in parentheses. Words or names preceded by a question mark and enclosed in parentheses were not clear from the original source but have been supplied as appropriate to the context. Other unattributed parenthetical notes within the body of an item originate with the source. Times within items are as given by the source. Passages in boldface or italics are as published.

SUBSCRIPTION/PROCUREMENT INFORMATION

The FBIS DAILY REPORT contains current news and information and is published Monday through Friday in eight volumes: China, East Europe, Soviet Union, East Asia, Near East & South Asia, Sub-Saharan Africa, Latin America, and West Europe. Supplements to the DAILY REPORTs may also be available periodically and will be distributed to regular DAILY REPORT subscribers. JPRS publications, which include approximately 50 regional, worldwide, and topical reports, generally contain less time-sensitive information and are published periodically.

Current DAILY REPORTs and JPRS publications are listed in *Government Reports Announcements* issued semimonthly by the National Technical Information Service (NTIS), 5285 Port Royal Road, Springfield, Virginia 22161 and the *Monthly Catalog of U.S. Government Publications* issued by the Superintendent of Documents, U.S. Government Printing Office, Washington, D.C. 20402.

The public may subscribe to either hardcover or microfiche versions of the DAILY REPORTs and JPRS publications through NTIS at the above address or by calling (703) 487-4630. Subscription rates will be provided by NTIS upon request. Subscriptions are available outside the United States from NTIS or appointed foreign dealers. New subscribers should expect a 30-day delay in receipt of the first issue.

U.S. Government offices may obtain subscriptions to the DAILY REPORTs or JPRS publications (hardcover or microfiche) at no charge through their sponsoring organizations. For additional information or assistance, call FBIS, (202) 338-6735,or write to P.O. Box 2604, Washington, D.C. 20013. Department of Defense consumers are required to submit requests through appropriate command validation channels to DIA, RTS-2C, Washington, D.C. 20301. (Telephone: (202) 373-3771, Autovon: 243-3771.)

Back issues or single copies of the DAILY REPORTs and JPRS publications are not available. Both the DAILY REPORTs and the JPRS publications are on file for public reference at the Library of Congress and at many Federal Depository Libraries. Reference copies may also be seen at many public and university libraries throughout the United States.